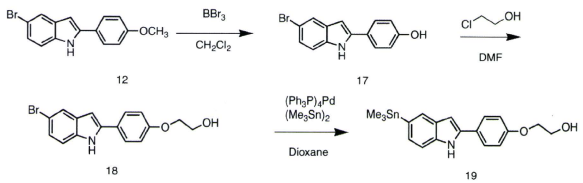

Scheme 4.

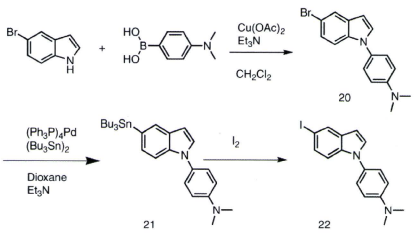

Scheme 5.

used as the starting materials for radioiodination in the preparation of [^{125}I]**5**, [^{125}I]**11**, [^{125}I]**14**, and [^{125}I]**16**. Novel radioiodinated 2-PI derivatives were obtained by iododestannylation reactions using NCS as an oxidant (Scheme 6). It was anticipated that not adding a carrier would result in a final product bearing a theoretical specific activity similar to that of ^{125}I (2200 Ci/mmol). The radiochemical identity of the radioiodinated ligands was verified by co-injection with non-radioiodinated compounds from HPLC profiles. The HPLC retention times are shown in Supplementary data. [^{125}I]**5**, [^{125}I]**11**, [^{125}I]**14**, and [^{125}I]**16** were each obtained in a radiochemical yield of 14–56% with a radiochemical purity of >95% after purification by HPLC.

The affinity of PI derivatives (**5**, **11**, **14**, **15**, **16**, and **22**) was evaluated based on inhibition of the binding of [^{125}I]IMPY to Aβ42 aggregates. The 2-PI derivatives (**5**, **11**, **14**, **15**, and **16**) showed inhibitory activity toward Aβ aggregates, while the 1-PI derivative **22** did not (Table 1 and Fig. 2). The K_i values of **5**, **11**, **14**, **15**, and **16** were 27, 4, 20, 33, and 26 nM, respectively, suggesting high affinity for Aβ(1–42) aggregates and considerable tolerance of structural modifications. They also suggested that the position of the substituted phenyl group in the PI molecule plays an important role in the affinity for Aβ aggregates.

To confirm the affinity of the 2-PI derivatives for Aβ plaques in the brain, fluorescent staining of sections of brain tissue from an animal model of AD was carried out with **11** (Fig. 3). Many specks of fluorescence were observed in brain sections of *Tg2576*

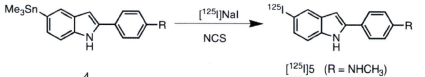

Scheme 6.

Table 1
Inhibition constants (K_i) for binding of PI derivatives determined using [^{125}I]IMPY as the ligand in Aβ(1–42) aggregates

Compound	K_i (nM)[a]
5	27.0 ± 0.18
11	4.24 ± 0.71
14	20.2 ± 5.15
15	32.9 ± 2.93
16	25.9 ± 5.13
22	>10,000

[a] Values are means ± standard error of the mean for 3–6 independent experiments.

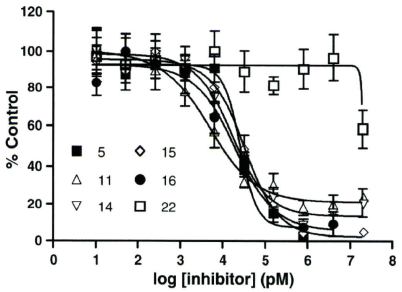

Figure 2. Curves of [^{125}I]IMPY against 2-PI (**5**, **11**, **14**, **15**, and **16**) and 1-PI (**22**).

transgenic mice (female, 28 months old) (Fig. 3A), while none were observed in wild-type mice (female, 22 months old) (Fig. 3B). The pattern of labeling was consistent with that observed with thioflavin S (Fig. 3C). Compound **11** should therefore show specific binding to Aβ plaques in the mouse brain. Compound **14** also clearly stained Aβ plaques in the *Tg2576* mouse brain (data not shown). A slight difference in K_i of **11** and **14** did not significantly affect the staining in mouse brain sections.

To evaluate the uptake into the brain of the PI derivatives, biodistribution experiments were performed in normal mice with four radioiodinated PI derivatives; [^{125}I]**5**, [^{125}I]**11**, [^{125}I]**14**, and [^{125}I]**16** (Table 2). Radioactivity penetrated the blood–brain barrier with the rate of uptake ranging from 1.2% to 2.6% ID/g brain at 2–10 min postinjection. But the washout of these probes from the brain in normal mice appears to be relatively slow. The uptake of [^{125}I]**11** was higher in the stomach than in any other organ, possibly due to deiodination. The brain uptake and clearance is similar to that of radioiodinated ThT analogs such as TZDM and IBOX.[13,14] More recently, we have developed ^{11}C-labeled phenylbenzofuran derivative, which are less lipophilic by replacing the iodine with a

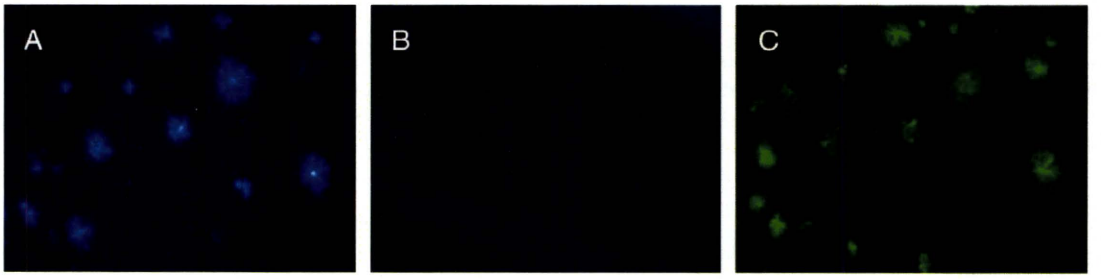

Figure 3. Neuropathological staining of **11** in 10-μm AD model mouse sections (A) and wild-type mouse sections (B). Labeled plaques were confirmed by staining of the adjacent sections with thioflavin S (C).

Table 2
Biodistribution of radioactivity after injection of [^{125}I]2-PI derivatives in normal mice[a]

Tissue	Time after injection (min)			
	2	10	30	60
[^{125}I]**5**				
Blood	3.77 (1.25)	1.71 (0.15)	1.36 (0.15)	0.80 (0.13)
Liver	22.85 (9.60)	26.83 (1.28)	23.07 (2.33)	15.89 (6.13)
Kidney	5.53 (1.77)	4.31 (0.44)	3.84 (0.67)	2.61 (0.86)
Intestine	0.97 (0.33)	3.57 (0.34)	8.54 (1.80)	9.48 (1.88)
Spleen	7.83 (2.24)	19.67 (8.82)	10.34 (1.26)	5.89 (3.27)
Pancreas	2.31 (0.70)	2.87 (0.33)	2.12 (0.32)	1.27 (0.23)
Heart	5.68 (1.27)	3.59 (0.29)	2.96 (0.42)	1.88 (0.57)
Stomach[b]	0.52 (0.03)	1.34 (0.53)	2.55 (2.12)	1.68 (0.53)
Brain	1.10 (0.27)	1.68 (0.13)	1.42 (0.03)	0.83 (0.17)
[^{125}I]**11**				
Blood	6.18 (0.65)	4.53 (0.37)	3.68 (0.41)	3.29 (1.00)
Liver	10.20 (1.92)	5.14 (1.01)	3.55 (0.62)	3.24 (0.76)
Kidney	9.49 (1.61)	4.46 (0.71)	4.58 (1.24)	4.71 (2.44)
Intestine	1.80 (0.24)	3.09 (0.40)	4.52 (0.58)	6.08 (1.58)
Spleen	4.13 (0.64)	3.28 (0.57)	2.60 (0.41)	2.24 (0.64)
Pancreas	5.21 (2.50)	4.13 (0.67)	3.10 (0.41)	2.30 (0.54)
Heart	8.08 (1.59)	4.82 (0.67)	1.87 (0.21)	1.84 (0.76)
Stomach[b]	4.03 (0.65)	10.65 (2.18)	17.77 (2.04)	16.26 (3.52)
Brain	1.19 (0.34)	1.19 (0.30)	0.96 (0.17)	0.71 (0.19)
[^{125}I]**14**				
Blood	3.59 (1.41)	1.97 (0.54)	1.38 (0.25)	0.74 (0.37)
Liver	17.81 (5.73)	13.96 (4.21)	10.38 (2.64)	8.22 (1.87)
Kidney	8.76 (2.19)	4.96 (1.44)	2.89 (0.44)	2.05 (0.54)
Intestine	1.90 (0.66)	6.85 (1.86)	12.32 (3.65)	20.35 (5.86)
Spleen	4.22 (0.78)	3.43 (1.15)	2.96 (0.41)	2.02 (0.92)
Pancreas	4.54 (0.44)	3.94 (1.46)	1.95 (0.33)	1.29 (0.37)
Heart	7.72 (1.94)	2.97 (1.26)	1.47 (0.20)	1.06 (0.42)
Stomach[b]	0.72 (0.39)	1.38 (1.42)	2.67 (3.24)	3.06 (1.28)
Brain	2.11 (0.69)	2.07 (0.71)	1.36 (0.37)	1.16 (0.32)
[^{125}I]**16**				
Blood	4.07 (0.30)	1.60 (0.30)	1.26 (0.26)	0.80 (0.20)
Liver	17.69 (2.64)	16.77 (2.20)	13.42 (1.70)	8.17 (1.28)
Kidney	11.93 (1.83)	9.35 (0.46)	6.77 (0.83)	2.76 (0.45)
Intestine	1.97 (0.22)	5.76 (0.66)	11.32 (1.65)	18.98 (3.21)
Spleen	7.56 (1.24)	7.09 (1.60)	4.75 (0.82)	2.39 (0.52)
Pancreas	5.55 (1.00)	5.59 (0.56)	3.57 (0.40)	2.22 (0.29)
Heart	12.91 (2.16)	5.84 (0.36)	2.97 (0.62)	1.36 (0.17)
Stomach[b]	0.97 (0.31)	1.97 (1.05)	2.11 (0.26)	1.62 (0.44)
Brain	2.13 (0.54)	2.62 (0.21)	1.93 (0.18)	1.82 (0.35)

[a] Expressed as % injected dose per gram. Each value represents the mean (SD) for 3–5 animals.
[b] Expressed as % injected dose per organ.

hydroxy group.[18] [^{11}C]Phenylbenzofuran, which has less lipophilicity than [^{125}I]phenylbenzofuran, showed a higher and faster peak of brain uptake and faster washout in normal mice. The improved properties of [^{11}C]phenylbenzofuran derivatives could make them a better candidate for the imaging of Aβ plaques. Similar to [^{125}I]phenylbenzofuran, the 2-PI derivatives had unfavorable in vivo pharmacokinetics in normal mice, despite their good affinity for Aβ aggregates. Additional structural changes, that is, reducing the lipophilicity by introducing a hydrophilic group, are necessary to improve the properties of 2-PI derivatives.

3. Conclusion

We developed PI derivatives as novel SPECT ligands for imaging Aβ plaques in the AD brain. 2-PI derivatives (**5**, **11**, **14**, **15**, and **16**) displayed excellent affinity for Aβ in binding experiments in vitro. They clearly stained Aβ plaques in *Tg2576* mouse brain, reflecting their affinity for Aβ aggregates in vitro. The degree to which the 2-PI derivatives penetrated the brain was very encouraging. However, non-specific binding in vivo reflected by a slow washout from the normal mouse brain may make them unsuitable for the imaging of Aβ plaques. In in vivo biodistribution results in normal mice indicate that there is a critical need to fine-tune the kinetics of brain uptake and washout. Additional changes to 2-PI may lead to useful probes for detecting Aβ plaques in the AD brain.

4. Experimental

4.1. General

All reagents were commercial products and used without further purification unless otherwise indicated. ^{1}H NMR spectra were obtained on a Varian Gemini 300 spectrometer with TMS as an internal standard. Coupling constants are reported in hertz. Multiplicity was defined by s (singlet), d (doublet), t (triplet), and m (multiplet). Mass spectra were obtained on a JEOL IMS-DX.

4.1.1. 4-Ethynyl-*N*-methylbenzenamine (1)

To a solution of 4-ethynylaniline (819 mg, 7 mmol) in DMSO were added methyl iodide (1.3 mL, 21 mmol) and anhydrous K_2CO_3 (4.8 g, 35 mmol). The reaction mixture was stirred at room temperature for 3 h. After it was poured into water, the mixture was extracted with ethyl acetate. The organic layers were dried over Na_2SO_4. The solvent was removed and the residue was purified by silica gel chromatography (hexane/ethyl acetate = 2:1) to give 313 mg of **1** (34.1%). ^{1}H NMR (300 MHz, $CDCl_3$) δ 2.49 (s, 1H), 2.83 (s, 3H), (s, 1H), 6.50 (d, J = 8.7 Hz, 2H), 7.32 (d, J = 8.7 Hz, 2H).

4.1.2. *N*-(4-Bromo-2-iodophenyl)acetamide (2)

A mixture of 4-bromo-2-iodoaniline (586 mg, 2 mmol) and acetic anhydride (0.19 mL, 2 mmol) in toluene (5 mL) was stirred at room temperature for 3.5 h. The solid that formed was filtered and washed with hexane to give 464 mg of **2** (69.4%). ^{1}H NMR (300 MHz, $CDCl_3$) δ 2.24 (s, 3H), 7.39 (s, 1H), 7.46 (dd, J = 2.4, 2.1 Hz, 1H), 7.90 (d, J = 2.1 Hz, 1H), 8.13 (d, J = 8.7 Hz, 1H).

4.1.3. 4-(5-Bromo-1*H*-indol-2-yl)-*N*-methylbenzenamine (3)

A mixture of **1** (313 mg, 2.4 mmol), **2** (396 mg, 1.2 mmol), $PdCl_2(PPh_3)$ (60 mg, 0.06 mmol), CuI (50 mg, 0.22 mmol), THF

(5 mL), and TBAF (1 M solution in THF, 5 mL) was stirred under reflux for 5 h. After removal of the THF, the residue was diluted with water and extracted with ethyl acetate, and the organic phase was dried over Na_2SO_4. The solvent was removed and the residue was purified by silica gel chromatography (hexane/ethyl acetate = 2:1) to give 179 mg of **3** (49.5%). ^{1}H NMR (300 MHz, $CDCl_3$) δ 2.90 (s, 3H), 6.57 (d, J = 2.4 Hz, 1H), 6.67 (d, J = 8.7 Hz, 2H), 7.21 (s, 2H), 7.49 (d, J = 8.7 Hz, 2H), 7.69 (s, 1H) 8.25 (s, 1H).

4.1.4. *N*-Methyl-4-(5-(trimethylstannyl)-1*H*-indol-2-yl) benzenamine (4)

A mixture of **3** (179 mg, 0.59 mmol), $Pd(PPh_3)_4$ (88 mg, 0.077 mmol) and $(Me_3Sn)_2$ (198 mg, 0.6 mmol) in 1,4-dioxane (5 mL) was stirred under reflux for 3.5 h. The solvent was removed and the residue was purified by silica gel chromatography (hexane/ethyl acetate = 3:1) to give 6 mg of **4** (2.1%). ^{1}H NMR (300 MHz, $CDCl_3$) δ 0.30 (s, 9H), 2.88 (s, 3H), 3.84 (s, 1H), 6.62 (s, 1H), 6.67 (d, J = 8.7 Hz, 2H), 7.22 (d, J = 9.0 Hz, 1H), 7.37 (d, J = 7.8 Hz, 1H), 7.50 (d, J = 9.0 Hz, 2H), 7.70 (s, 1H), 8.18 (s, 1H).

4.1.5. 4-(5-Iodo-1*H*-indol-2-yl)-*N*-methylbenzenamine (5)

To a solution of **4** (9 mg, 0.019 mmol) in ethyl acetate (1 mL) was added a solution of iodine in ethyl acetate (1 mL, 0.25 M) at room temperature. The mixture was stirred for 15 s, and $NaHSO_3$ solution (1 mL) was added. The organic phase was separated and dried over Na_2SO_4. The solvent was removed and the residue was purified by silica gel chromatography (hexane/ethyl acetate = 3:1) to give 5 mg of **5** (77.4%). ^{1}H NMR (300 MHz, $CDCl_3$) δ 2.89 (s, 3H), 6.56 (s, 1H), 6.67 (d, J = 8.7 Hz, 2H), 7.13 (d, J = 8.1 Hz, 1H), 7.37 (dd, J = 1.8, 1.8 Hz, 1H), 7.48 (d, J = 9.0 Hz, 1H) 7.90 (s, 1H), 8.23 (s, 1H). HRMS m/z $C_{15}H_{13}N_2I$ found 348.0109/calcd 348.0123 (M^+).

4.1.6. 4-(5-Bromo-1*H*-indol-2-yl)-*N*,*N*-dimethylbenzenamine (6)

The same reaction as described above to prepare **3** was used, and 25 mg of **6** was obtained in a 27.2% yield from **2** (99 mg, 0.3 mmol) and 4-ethynyl-*N*,*N*-dimethylaniline (65 mg, 0.45 mmol). ^{1}H NMR (300 MHz, $CDCl_3$) δ 3.02 (s, 6H), 6.59 (d, J = 1.8 Hz, 1H), 6.78 (d, J = 9.0 Hz, 2H), 7.21–7.22 (m, 2H), 7.53 (d, J = 9.0 Hz, 2H), 7.68 (s, 1H) 8.27 (s, 1H).

4.1.7. *N*,*N*-Dimethyl-4-(5-(trimethylstannyl)-1*H*-indol-2-yl) benzenamine (7)

The same reaction as described above to prepare **4** was used, and 2 mg of **7** was obtained in a 7.1% yield from **6** (22 mg, 0.07 mmol). ^{1}H NMR (300 MHz, $CDCl_3$) δ 0.31 (s, 9H), 3.01 (s, 6H), 6.64 (s, 1H), 6.79 (d, J = 9.3 Hz, 2H), 7.23 (d, J = 6.9 Hz, 1H), 7.38 (d, J = 8.1 Hz, 1H), 7.55 (d, J = 9.0 Hz, 2H), 7.71 (s, 1H), 8.21 (s, 1H).

4.1.8. *tert*-Butyl 5-bromo-2-(4-(dimethylamino)phenyl)-1*H*-indole-1-carboxylate (8)

$(Boc)_2O$ (159 mg, 0.73 mmol) was added to a solution of **7** (41 mg, 0.13 mmol) and 4-(*N*,*N*-dimethylamino)pyridine (DMAP) (4.8 mg, 0.004 mmol) in acetonitrile. The reaction mixture was stirred at room temperature for 3 h. After it was poured into water, the mixture was extracted with ethyl acetate. The organic layers were dried over Na_2SO_4. The solvent was removed and the residue was purified by silica gel chromatography (hexane/ethyl acetate = 4:1) to give 54 mg of **8** (100%). ^{1}H NMR (300 MHz, $CDCl_3$) δ 1.38 (s, 9H), 3.00 (s, 6H), 6.41 (s, 1H), 6.75 (d, J = 8.4 Hz, 2H), 7.29 (s, 2H), 7.36 (d, J = 9.0 Hz, 1H), 7.63 (s, 1H) 8.02 (d, J = 8.7 Hz, 1H).

4.1.9. *tert*-Butyl 5-(tributylstannyl)-2-(4-(dimethylamino) phenyl)-1*H*-indole-1-carboxylate (9)

A mixture of **8** (54 mg, 0.13 mmol), $(Bu_3Sn)_2$ (0.3 mL) and $(Ph_3P)_4Pd$ (16 mg, 0.01 mmol) in a mixed solvent (6 mL, 1:1 = 1,4-dioxane/Et_3N) was stirred under reflux for 11 h. The solvent was removed, and the residue was purified by silica gel chromatography (hexane/ethyl acetate = 9:1) to give 20 mg of **9** (12.4%). ^{1}H NMR (300 MHz, $CDCl_3$) δ 0.84–1.61 (m, 36H), 2.99 (s, 6H), 6.46 (s, 1H), 6.75 (d, J = 8.7 Hz, 2H), 7.29 (d, J = 8.4 Hz, 2H), 7.35 (d, J = 8.1 Hz, 1H), 7.61 (s, 1H), 8.11 (d, J = 7.5 Hz, 1H).

4.1.10. *tert*-Butyl 2-(4-(dimethylamino)phenyl)-5-iodo-1*H*-indole-1-carboxylate (10)

The same reaction as described above to prepare **5** was used, and 10 mg of **10** was obtained in a 67.6% yield from **9** (20 mg, 0.03 mmol). ^{1}H NMR (300 MHz, $CDCl_3$) δ 1.37 (s, 9H), 3.00 (s, 3H), 6.39 (s, 1H), 6.74 (d, J = 8.7 Hz, 2H), 7.29 (s, 2H), 7.53 (dd, J = 1.8, 1.8 Hz, 1H) 7.84 (d, J = 2.1 Hz, 1H), 7.91 (d, J = 9.0 Hz, 1H).

4.1.11. 4-(5-Iodo-1*H*-indol-2-yl)-*N*,*N*-dimethylbenzenamine (11)

To a solution of **10** (71 mg, 0.15 mmol) in CH_2Cl_2 (2 mL) was added TFA (300 μL) at room temperature. After the mixture was stirred for 3 h, the solvent was removed. The residue was purified by preparative TLC (hexane/ethyl acetate = 3:1) to give 13 mg of **11** (27.0%). ^{1}H NMR (300 MHz, $CDCl_3$) δ 3.02 (s, 6H), 6.57 (s, 1H), 6.79 (d, J = 8.7 Hz, 2H), 7.14 (d, J = 8.7 Hz, 1H), 7.36 (dd, J = 1.5, 1.5 Hz, 1H), 7.53 (d, J = 9.0 Hz, 1H), 7.89 (s, 1H), 8.28 (s, 1H). HRMS m/z $C_{16}H_{15}N_2I$ found 362.0278/calcd 362.0280 (M^+).

4.1.12. 5-Bromo-2-(4-methoxyphenyl)-1*H*-indole (12)

The same reaction as described above to prepare **3** was used, and 54 mg of **12** was obtained in a 30.7% yield from **2** (198 mg, 0.6 mmol) and *p*-ethynylanisole (116 μL, 0.9 mmol). ^{1}H NMR (300 MHz, $CDCl_3$) δ 3.87 (s, 3H), 6.50 (s, 1H), 6.99 (d, J = 8.7 Hz, 2H), 7.25 (s, 2H), 7.59 (d, J = 8.7 Hz, 2H), 7.12 (s, 1H), 8.30 (s, 1H).

4.1.13. 2-(4-Methoxyphenyl)-5-(trimethylstannyl)-1*H*-indole (13)

The same reaction as described above to prepare **4** was used, and 15 mg of **13** was obtained in a 23.9% yield from **12** (49 mg, 0.16 mmol). ^{1}H NMR (300 MHz, $CDCl_3$) δ 0.30 (s, 9H), 3.86 (s, 3H), 6.68 (s, 1H), 6.98 (d, J = 9.0 Hz, 2H), 7.26 (d, J = 7.2 Hz, 1H), 7.39 (d, J = 7.8 Hz, 1H), 7.59 (d, J = 9.0 Hz, 2H), 7.73 (s, 1H), 8.22 (s, 1H).

4.1.14. 5-Iodo-2-(4-methoxyphenyl)-1*H*-indole (14)

The same reaction as described above to prepare **5** was used, and 9 mg of **14** was obtained in a 66.3% yield from **13** (15 mg, 0.039 mmol). ^{1}H NMR (300 MHz, $CDCl_3$) δ 3.86 (s, 3H), 6.63 (s, 1H), 6.99 (d, J = 9.0 Hz, 2H), 7.16 (d, J = 8.4 Hz, 1H), 7.41 (dd, J = 1.8, 1.5 Hz, 1H), 7.58 (d, J = 8.7 Hz, 2H), 7.93 (s, 1H), 8.29 (s, 1H). HRMS m/z $C_{15}H_{12}NOI$ found 348.9962/calcd 348.9964 (M^+).

4.1.15. 4-(5-Iodo-1*H*-indol-2-yl)phenol (15)

BBr_3 (0.7 mL, 1 M solution in CH_2Cl_2) was added to a solution of **14** (80 mg, 0.23 mmol) in CH_2Cl_2 (5 mL) dropwise in an ice bath. The mixture was allowed to warm to room temperature and stirred for 24 h. Water was added while the reaction mixture was cooled in an ice bath. The mixture was extracted with $CHCl_3$ and the water layer was extracted with ethyl acetate. The organic phase was dried over Na_2SO_4 and filtered. The solvent was removed, and the residue was purified by silica gel chromatography (hexane/ethyl acetate = 4:1) to give 15 mg of **15** (19.5%). ^{1}H NMR (300 MHz, CD_3OD) δ 6.57 (s, 1H), 6.76 (d, J = 8.7 Hz, 2H), 7.16 (d, J = 8.7 Hz, 1H), 7.29 (dd, J = 1.5, 1.5 Hz, 1H), 7.60 (d, J = 8.7 Hz, 2H), 7.81 (s, 1H). HRMS m/z $C_{14}H_{10}NOI$ found 334.9808/calcd 334.9807 (M^+).

4.1.16. 2-(4-(5-Iodo-1*H*-indol-2-yl)phenoxy)ethanol (16)

A mixture of **15** (13 mg, 0.039 mmol), potassium carbonate (48 mg, 0.12 mmol) and ethylene chlorohydrin (4 μL, 0.06 mmol) in anhydrous DMF (3 mL) was stirred under reflux for 10.5 h. After cooling to room temperature, water was added, and the reaction mixture was extracted with $CHCl_3$. The organic layer was separated, dried over Na_2SO_4 and evaporated. The resulting residue was purified by preparative TLC (hexane/ethyl acetate = 1:1) to give 3 mg of **16** (20.4%). ^1H NMR (300 MHz, CD_3OD) δ 3.89 (t, J = 9.6 Hz, 2H), 4.09 (t, J = 9.3 Hz, 2H), 6.62 (s, 1H), 7.02 (d, J = 8.7 Hz, 2H), 7.17 (d, J = 8.1 Hz, 1H), 7.30 (dd, J = 1.8, 1.5 Hz, 1H), 7.70 (d, J = 9.0 Hz, 2H), 7.82 (s, 1H), 11.0 (s, 1H). HRMS m/z $C_{16}H_{14}NO_2I$ found 379.0078/calcd 379.0069 (M^+).

4.1.17. 4-(5-Bromo-1*H*-indol-2-yl)phenol (17)

The same reaction as described above to prepare **15** was used, and 13 mg of **17** was obtained in a 13.0% yield from **13** (105 mg, 0.347 mmol). ^1H NMR (300 MHz, CD_3OD) δ 6.58 (s, 1H), 6.84 (d, J = 9.0 Hz, 2H), 7.11 (dd, J = 1.8, 1.5 Hz, 1H), 7.25 (d, J = 8.7 Hz, 1H), 7.60 (d, J = 9.0 Hz, 3H).

4.1.18. 2-(4-(5-Bromo-1*H*-indol-2-yl)phenoxy)ethanol (18)

The same reaction as described above to prepare **16** was used, and 1.8 mg of **18** was obtained in a 14.2% yield from **17** (11 mg, 0.038 mmol). ^1H NMR (300 MHz, CD_3OD) δ 3.89 (t, J = 8.7 Hz, 2H), 4.09 (t, J = 9.6 Hz, 2H), 6.64 (s, 1H), 7.02 (d, J = 8.7 Hz, 2H), 7.13 (dd, J = 1.5, 1.5 Hz, 1H), 7.26 (d, J = 8.7 Hz, 1H), 7.61 (s, 1H), 7.70 (d, J = 8.7 Hz, 2H).

4.1.19. 2-(4-(5-(Trimethylstannyl)-1*H*-indol-2-yl)phenoxy) ethanol) (19)

The same reaction as described above to prepare **4** was used, and 9 mg of **19** was obtained in a 89.8% yield from **18** (8 mg, 0.02 mmol). ^1H NMR (300 MHz, $CDCl_3$) δ 0.31 (s, 9H), 3.99 (t, J = 8.7 Hz, 2H), 4.14 (t, J = 9.3 Hz, 2H), 6.71 (d, J = 11.1 Hz, 1H), 6.76 (d, J = 9.3 Hz, 1H). 6.98–7.08 (m, 2H), 7.39 (s, 1H), 7.57–7.62 (m, 2H), 7.88 (d, J = 9.3 Hz, 1H), 8.25 (s, 1H).

4.1.20. 4-(5-Bromo-1*H*-indol-1-yl)-*N*,*N*-dimethylbenzenamine (20)

A mixture of 5-bromoindole (100 mg, 0.51 mmol), 4-(dimethylamino)-phenylboronic acid (84 mg, 0.51 mmol), $Cu(OAc)_2$ (200 mg, 1.00 mmol), triethylamine (0.18 mL), and powdered molecular sieves 3 Å was suspended in CH_2Cl_2 (10 mL), and stirred for 1 h. The solvent was removed, and the residue was purified by silica gel chromatography (hexane/ethyl acetate = 9:1) to give 71 mg of **20** (44.2%). ^1H NMR (300 MHz, $CDCl_3$) δ 3.02 (s, 6H), 6.55 (d, J = 2.7 Hz, 1H), 6.82 (d, J = 9.0 Hz, 2H), 7.28 (d, J = 1.8 Hz, 1H) 7.78 (d, J = 1.2 Hz, 1H).

4.1.21. 4-(5-(Tributylstannyl)-1*H*-indol-1-yl)-*N*,*N*-dimethylbenzenamine (21)

The same reaction as described above to prepare **9** was used, and 21 mg of **21** was obtained in a 12.4% yield from **20** (102 mg, 0.32 mmol). ^1H NMR (300 MHz, $CDCl_3$) δ 0.87–1.56 (m, 27H), 3.02 (s, 6H), 6.61 (d, J = 3.3 Hz, 1H), 6.82 (d, J = 9.0 Hz, 2H), 7.24 (d, J = 3.0 Hz, 2H), 7.34 (d, J = 8.7 Hz, 2H), 7.45 (d, J = 3.0 Hz, 1H), 7.77 (s, 1H).

4.1.22. 4-(5-Iodo-1*H*-indol-1-yl)-*N*,*N*-dimethylbenzenamine (22)

The same reaction as described above to prepare **5** was used, and 8 mg of **22** was obtained in a 55.3% yield from **21** (21 mg, 0.04 mmol). ^1H NMR (300 MHz, $CDCl_3$) δ 3.02 (s, 6H), 6.54 (d, J = 3.3 Hz, 1H), 6.81 (d, J = 6.6 Hz, 2H), 7.20 (d, J = 7.8 Hz, 2H), 7.29 (d, J = 9.0 Hz, 2H), 7.41 (dd, J = 1.5, 1.8 Hz, 1H), 7.99 (d, J = 1.2 Hz, 1H). HRMS m/z $C_{16}H_{15}N_2I$ found 362.0287/calcd 362.0280 (M^+).

4.2. Iododestannylation reaction

The radioiodinated forms of compounds **5**, **11**, **14**, and **16** were prepared from the corresponding trimethyltin derivatives by iododestannylation using the previously described *N*-chlorosuccinimide (NCS) method, with some modifications.[26] Briefly, a 80 μL solution of **5**, **11**, **14**, and **16** in methanol containing 1% acetic acid (0.56 mg/mL) was mixed with 20 μL of NCS in methanol (0.5 mg/mL) in a sealed vial, and [^{125}I]NaI (0.1–0.2 mCi, specific activity 2200 Ci/mmol) was added. The reaction was allowed to proceed at room temperature for 20 s and terminated by addition of $NaHSO_3$. After extraction with ethyl acetate, the extract was dried by passing through an anhydrous Na_2SO_4 column and blown dry with a stream of nitrogen gas. The radioiodinated ligand was purified by HPLC on a Cosmosil C_{18} column with an isocratic solvent of H_2O/acetonitrile (4:6–1:1) at a flow rate of 1.0 mL/min.

4.3. Binding assays using the aggregated Aβ peptide in solution

A solid form of Aβ42 was purchased from Peptide Institute (Osaka, Japan). Aggregation was carried out by gently dissolving the peptide (0.25 mg/mL) in a buffer solution (pH 7.4) containing 10 mM sodium phosphate and 1 mM EDTA. The solution was incubated at 37 °C for 42 h with gentle and constant shaking. Binding assays were carried out as described previously.[27] [^{125}I]IMPY (6-iodo-2-(4′-dimethylamino)phenyl-imidazo[1,2]pyridine) with 2200 Ci/mmol specific activity and greater than 95% radiochemical purity was prepared using the standard iododestannylation reaction as described previously.[15] Binding assays were carried out in 12 × 75 mm borosilicate glass tubes. A mixture containing 50 μL of test compound (0.2 pM–400 nM in 10% EtOH), 50 μL of [^{125}I]IMPY (0.02 nM diluted in 50% EtOH), 50 μL of Aβ42 aggregates, and 850 μL of 10% ethanol was incubated at room temperature for 3 h. The mixture was then filtered through Whatman GF/B filters using a Brandel M-24 cell harvester, and the filters containing the bound ^{125}I ligand were placed in a gamma counter (Aloka, ARC-380). Values for the half-maximal inhibitory concentration (IC_{50}) were determined from displacement curves of three independent experiments using GraphPad Prism 4.0, and those for the inhibition constant (K_i) were calculated using the Cheng–Prusoff equation.[28]

4.4. Neuropathological staining of mouse brain sections

The experiments with animals were conducted in accordance with our institutional guidelines and approved by the Nagasaki University Animal Care Committee. *Tg2576* transgenic mice (female, 28 months old) and wild-type mice (female, 22 months old) were used as the Alzheimer's model and control, respectively. After the mice were sacrificed by decapitation, the brain was immediately removed and frozen in powdered dry ice. The frozen blocks were sliced into serial sections, 10 μm thick. Each slide was incubated with a 50% EtOH solution (100 μM) of compounds **11** and **14** for 10 min. The sections were washed in 50% EtOH for 1 min two times, and examined using a microscope (KEYENCE BZ-8100) equipped with a DAPI-BP filter set (excitation, 360 nm; diachromic mirror, 400 nm; longpass filter, 460 nm). Thereafter, the sections were also stained with thioflavin S, a pathological dye commonly used for staining Aβ plaques in the brain, and examined using a microscope (KEYENCE BZ-8100) equipped with a GFP-BP filter set (excitation, 470 nm; diachromic mirror, 495 nm; longpass filter, 535 nm).

4.5. In vivo biodistribution in normal mice

A saline solution (100 μL) of radiolabeled agents (0.2–0.4 μCi) containing ethanol (10 μL) was injected intravenously directly into the tail of ddY mice (5 weeks old, 25–30 g). The mice were sacrificed at various time points postinjection. The organs of interest were removed and weighed, and the radioactivity was measured with an automatic gamma counter (Aloka, ARC-380 or Perkin-Elmer 2470 wizard2).

Acknowledgments

The study was supported by a Grants-in Aid for Young Scientists (A) and Exploratory Research from the Ministry of Education, Culture, Sports, Science and Technology, the Program for Promotion of Fundamental Biomedical Innovation (NIBIO), and a Health Labor Sciences Research Grant.

Supplementary data

Supplementary data associated with this article can be found, in the online version, at doi:10.1016/j.bmc.2010.05.013.

References and notes

1. Klunk, W. E. *Neurobiol. Aging* **1998**, *19*, 145.
2. Selkoe, D. J. *Phys. Rev.* **2001**, *81*, 741.
3. Mathis, C. A.; Lopresti, B. J.; Klunk, W. E. *Nucl. Med. Biol.* **2007**, *34*, 809.
4. Mathis, C. A.; Wang, Y.; Klunk, W. E. *Curr. Pharm. Des.* **2004**, *10*, 1469.
5. Nordberg, A. *Lancet Neurol.* **2004**, *3*, 519.
6. Ono, M.; Wilson, A.; Norbrega, J.; Westaway, D.; Verhoeff, P.; Zhuang, Z. P.; Kung, M. P.; Kung, H. F. *Nucl. Med. Biol.* **2003**, *30*, 565.
7. Rowe, C. C.; Ackerman, U.; Browne, W.; Mulligan, R.; Pike, K. L.; O'Keefe, G.; Tochon-Danguy, H.; Chan, G.; Berlangieri, S. U.; Jones, G.; Dickinson-Rowe, K. L.; Kung, H. P.; Zhang, W.; Kung, M. P.; Skovronsky, D.; Dyrks, T.; Holl, G.; Krause, S.; Friebe, M.; Lehman, L.; Lindemann, S.; Dinkelborg, L. M.; Masters, C. L.; Villemagne, V. L. *Lancet Neurol.* **2008**, *7*, 129.
8. Choi, S. R.; Golding, G.; Zhuang, Z.; Zhang, W.; Lim, N.; Hefti, F.; Benedum, T. E.; Kilbourn, M. R.; Skovronsky, D.; Kung, H. F. *J. Nucl. Med.* **2009**, *50*, 1887.
9. Mathis, C. A.; Wang, Y.; Holt, D. P.; Huang, G. F.; Debnath, M. L.; Klunk, W. E. *J. Med. Chem.* **2003**, *46*, 2740.
10. Klunk, W. E.; Engler, H.; Nordberg, A.; Wang, Y.; Blomqvist, G.; Holt, D. P.; Bergstrom, M.; Savitcheva, I.; Huang, G. F.; Estrada, S.; Ausen, B.; Debnath, M. L.; Barletta, J.; Price, J. C.; Sandell, J.; Lopresti, B. J.; Wall, A.; Koivisto, P.; Antoni, G.; Mathis, C. A.; Langstrom, B., et al *Ann. Neurol.* **2004**, *55*, 306.
11. Johnson, A. E.; Jeppsson, F.; Sandell, J.; Wensbo, D.; Neelissen, J. A. M.; Juréus, A.; Ström, P.; Norman, H.; Farde, L.; Svensson, *S. J. Neurochem.* **2009**, *108*, 1177.
12. Nyberg, S.; Jönhagen, M. E.; Cselényi, Z.; Halldin, C.; Julin, P.; Olsson, H.; Freund-Levi, Y.; Andersson, J.; Varnäs, K.; Svensson, S.; Farde, L. *Eur. J. Nucl. Med. Mol. Imaging* **2009**, *11*, 1859.
13. Zhuang, Z. P.; Kung, M. P.; Hou, C.; Skovronsky, D.; Gur, T. L.; Trojanowski, J. Q.; Lee, V. M. Y.; Kung, H. F., et al *J. Med. Chem.* **2001**, *44*, 1905.
14. Zhuang, Z. P.; Kung, M. P.; Hou, C.; Plossel, K.; Skovronsky, D.; Gur, T. L.; Trojanowski, J. Q.; Lee, V. M. Y.; Kung, H. F. *Nucl. Med. Biol.* **2001**, *28*, 887.
15. Kung, M. P.; Hou, C.; Zhuang, Z. P.; Zhang, B.; Skovronsky, D.; Trojanowski, J. Q.; Lee, V. M.; Kung, H. F. *Brain Res.* **2002**, *956*, 202.
16. Newberg, A. B.; Wintering, N. A.; Plossl, K.; Hochold, J.; Stabin, M. G.; Watson, M.; Skovronsky, D.; Clark, C. M.; Kung, M. P.; Kung, H. F. *J. Nucl. Med.* **2006**, *47*, 748.
17. Ono, M.; Kung, M. P.; Hou, C.; Kung, H. F. *Nucl. Med. Biol.* **2002**, *29*, 633.
18. Ono, M.; Kawashima, H.; Nonaka, A.; Kawai, T.; Haratake, M.; Mori, H.; Kung, M. P.; Kung, H. F.; Saji, H.; Nakayama, M. *J. Med. Chem.* **2006**, *49*, 2725.
19. Chang, Y. S.; Jeong, J. M.; Lee, Y. S.; Kim, H. W.; Rai, B. G.; Kim, Y. J.; Lee, D. S.; Chung, J. K.; Lee, M. C. *Nucl. Med. Biol.* **2006**, *33*, 811.
20. Cai, L.; Cuevas, J.; Temme, S.; Herman, M. M.; Dagostin, C.; Widdowson, D. A.; Innis, R. B.; Pike, V. W. *J. Med. Chem.* **2008**, *51*, 148.
21. Cai, L.; Liow, J. S.; Zoghbi, S. S.; Cuevas, J.; Baetas, C.; Hong, J.; Shetty, H. U.; Seneca, N. M.; Brown, A. K.; Gladding, R.; Temme, S. S.; Herman, M. M.; Innis, R. B.; Pike, V. W. *J. Med. Chem.* **2007**, *50*, 4746.
22. Zeng, F.; Alagille, D.; Tamagnan, G. D.; Brian J. Ciliax, B. J.; Levey, A. I.; Goodman, M. M. *ACS Med. Chem. Lett.* ASAP. doi:10.1021/ml100005j.
23. Dishino, D. D.; Welch, M. J.; Kilbourn, M. R.; Raichle, M. E. *J. Nucl. Med.* **1983**, *24*, 1030.
24. Suzuki, N.; Yasaki, S.; Yasuhara, A.; Sakamoto, T. *Chem. Pharm. Bull.* **2003**, *10*, 1170.
25. Sano, H.; Noguchi, T.; Tanatani, A.; Hashimoto, Y.; Miyachi, H. *Bioorg. Med. Chem.* **2005**, *13*, 3079.
26. Arano, Y.; Wakisaka, K.; Ohmoto, Y.; Uezono, T.; Akizawa, H.; Nakayama, M.; Sakahara, H.; Tanaka, C.; Konishi, J.; Yokoyama, A. *Bioconjugate Chem.* **1996**, *7*, 628.
27. Kung, M. P.; Hou, C.; Zhuang, Z. P.; Skovronsky, D.; Kung, H. F. *Brain Res.* **2004**, *1025*, 98.
28. Chang, Y.; Prisoff, W. *Biochem. Pharmacol.* **1973**, *22*, 3099.

ACS Chemical Neuroscience pubs.acs.org/acschemicalneuroscience

Synthesis and Evaluation of Novel Chalcone Derivatives with ^{99m}Tc/Re Complexes as Potential Probes for Detection of β-Amyloid Plaques

Masahiro Ono,*[,†,‡] Ryoichi Ikeoka,[†] Hiroyuki Watanabe,[†] Hiroyuki Kimura,[‡] Takeshi Fuchigami,[†] Mamoru Haratake,[†] Hideo Saji,[‡] and Morio Nakayama*[,†]

[†]Graduate School of Biomedical Sciences, Nagasaki University, 1-14 Bunkyo-machi, Nagasaki 852-8521, Japan, and [‡]Graduate School of Pharmaceutical Sciences, Kyoto University, 46-29 Yoshida Shimoadachi-cho, Sakyo-ku, Kyoto 606-8501, Japan

Abstract

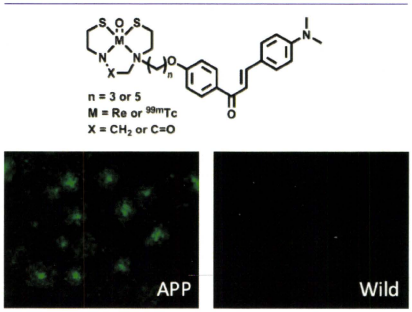

Four ^{99m}Tc-labeled chalcone derivatives and their corresponding rhenium analogues were tested as potential probes for imaging β-amyloid plaques. The chalcones showed higher affinity for Aβ(1−42) aggregates than did ^{99m}Tc complexes. In sections of brain tissue from an animal model of AD, the four Re chalcones intensely stained β-amyloid plaques. In biodistribution experiments using normal mice, ^{99m}Tc-BAT-chalcone ([^{99m}Tc]**17**) displayed high uptake in the brain (1.48% ID/g) at 2 min postinjection. The radioactivity washed out from the brain rapidly (0.17% ID/g at 60 min), a highly desirable feature for an imaging agent. [^{99m}Tc]**17** may be a potential probe for imaging β-amyloid plaques in Alzheimer's brains.

Keywords: Alzheimer's disease, β-amyloid plaque, ^{99m}Tc, single photon emission computed tomography (SPECT) imaging

Alzheimer's disease (AD), the most common senile dementia, is characterized by β-amyloid (Aβ) plaques, vascular amyloid, neurofibrillary tangles, and progressive neurodegeneration. The formation of plaques composed of β-amyloid peptides (Aβ) in the brain is considered the initial neurodegenerative event in AD (*1*). Thus, the detection of individual plaques *in vivo* by single photon emission tomography (SPECT) or positron emission tomography (PET) should improve diagnosis and also accelerate the discovery of effective therapeutic agents for AD (*2*−*4*).

Many radiolabeled probes for imaging β-amyloid based on Congo Red, thioflavin T, and DDNP have been reported. Among them, [^{11}C]PIB (*5*, *6*), [^{11}C]SB-13 (*7*, *8*), [^{18}F]BAY94-9172 (*9*, *10*), [^{11}C]BF-227 (*11*), [^{18}F]FDDNP (*12*, *13*), [^{123}I]IMPY (*14*−*16*), and [^{18}F]-AV-45 (*17*, *18*) have been tested clinically and demonstrated potential utility.

Recently, while searching for novel imaging probes, we found that ^{125}I-, ^{11}C-, and ^{18}F-labeled chalcone derivatives showed high affinity for Aβ aggregates and good uptake into and rapid clearance from the brain (*19*−*21*). In this study, we planned the development of novel chalcone derivatives labeled with technetium-99m (^{99m}Tc). ^{99m}Tc ($T_{1/2}$ = 6.01 h, 141 keV) has become the most commonly used radionuclide in diagnostic nuclear medicine for several reasons: it is readily produced by a ^{99}Mo/^{99m}Tc generator, the medium gamma-ray energy it emits is suitable for detection, and its physical half-life is compatible with the biological localization and residence time required for imaging. It is ready availability, essentially 24 h/day, and ease of use make it the radionuclide of choice. New ^{99m}Tc-labeled imaging agents will provide simple, convenient, and widespread SPECT-based imaging methods for detecting and eventually quantifying β-amyloid plaques in living brain tissue.

Kung et al. reported that a dopamine transporter imaging agent, [^{99m}Tc]TRODAT-1, is useful to detect the loss of dopamine neurons in the basal ganglia associated with Parkinson's disease. This is the first example of a ^{99m}Tc imaging agent that can penetrate the blood−brain barrier via a simple diffusion mechanism and localize at sites in the central nervous system. Based on this success, efforts were made to search for comparable ^{99m}Tc imaging

Received Date: April 27, 2010
Accepted Date: June 25, 2010
Published on Web Date: July 08, 2010

DOI: 10.1021/cn100042d | ACS Chem. Neurosci. (2010), 1, 598–607

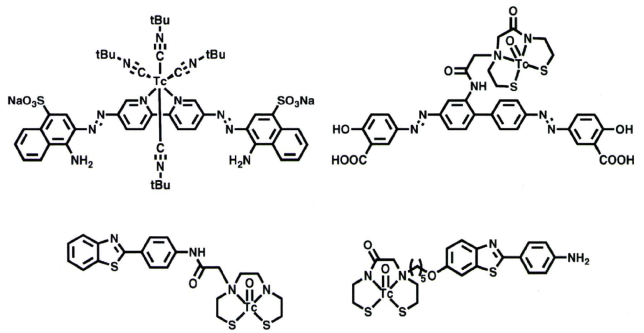

Figure 1. Chemical structure of ^{99m}Tc-labeled Aβ imaging probes reported previously.

Scheme 1. Synthesis of Chelation Ligands

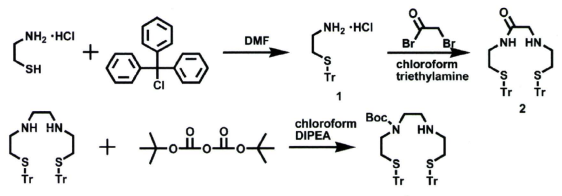

agents that target binding sites on β-amyloid plaques in the brain of AD patients. Several ^{99m}Tc-labeled imaging probes have been developed (Figure 1), but no clinical study of them has been reported (*22*−*25*).

In the present study, to develop more useful ^{99m}Tc-labeled probes for clinical diagnosis, we synthesized four chalcone derivatives with monoamine−monoamide dithiol (MAMA) and bis-amino-bis-thiol (BAT). MAMA and BAT were selected as chelation ligands taking into consideration the permeability of the blood−brain barrier, because they form an electrically neutral complex with ^{99m}Tc (*26*). We then evaluated their biological potential as probes by testing their affinity for Aβ aggregates and β-amyloid plaques in sections of brain tissue from Tg2576 mice and their uptake by and clearance from the brain in biodistribution experiments using normal mice. To our knowledge, this is the first time chalcones with ^{99m}Tc/Re complexes have been proposed as probes for the detection of β-amyloid plaques in the brain.

Results and Discussion

The synthesis of the ^{99m}Tc/Re chalcone derivatives is outlined in Schemes 1−3. The chelation ligands (MAMA and BAT) were synthesized according to methods reported previously with some slight modifications (Scheme 1) (*26*). The most useful method of preparing chalcones is the condensation of acetophenones with benzaldehydes(*19*). In this process, 4-hydroxybenzaldehyde was reacted with 4-dimethylaminobenzaldehyde in the presence of a basic catalyst (10% KOH) in ethanol at room temperature to form 4-dimethylamino-4′-hydroxy-chalcone (**4**) in a yield of 70%. The reaction of dibromo with **4** produced two chalcone derivatives (**5** and **6**) with alkyl groups (n = 3 or 5) of different lengths. Then, **5** (n = 5) or **6** (n = 3) was joined to **2** (Tr-MAMA) or **3** (Tr-Boc-BAT) to generate compounds **7** (n = 5) and **13** (n = 3) (Tr-MAMA-chalcones) or compounds **10** (n = 5) and **16** (n = 3) (Tr-Boc-BAT). Compounds **8**, **11**, **14**, and **17** (the precursors for ^{99m}Tc labeling) were obtained by deprotection of the thiol groups in **7**, **10**, **13**, and **16**, respectively. The Re complexes (**9**, **12**, **15**, and **18**) were prepared by the reaction of **7**, **11**, **13**, and **17** with $(PPh_3)_2ReOCl_3$. The corresponding ^{99m}Tc complexes, [^{99m}Tc]**8**, [^{99m}Tc]**11**, [^{99m}Tc]**14**, and [^{99m}Tc]**17**, were prepared by a ligand exchange reaction employing the precursor ^{99m}Tc-gluco-heptonate (GH). The resulting mixture was analyzed by reversed-phase HPLC, showing that a single radioactive complex formed with radiochemical purity higher than

DOI: 10.1021/cn100042d | ACS Chem. Neurosci. (2010), 1, 598–607

Scheme 2. Synthesis of Chalcone Derivatives

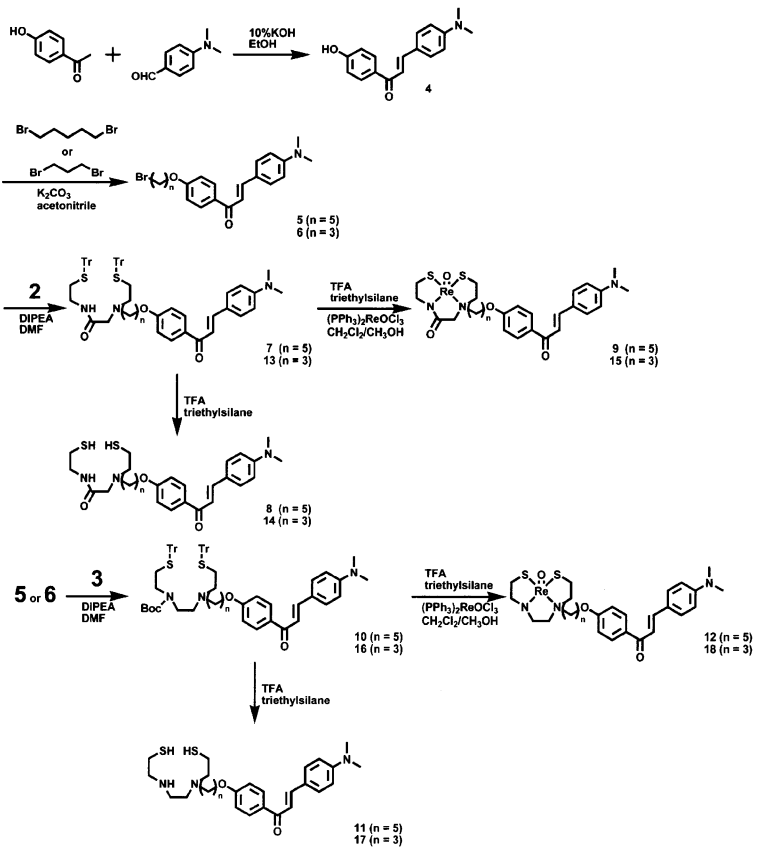

95% after purification by HPLC. The identity of the complex was established by comparative HPLC using the corresponding Re complexes as a reference (Table 1). The retention times for [^{99m}Tc]**8**, [^{99m}Tc]**11**, [^{99m}Tc]**14**, and [^{99m}Tc]**17** on HPLC (radioactivity) were 14.2, 20.3, 9.3, and 12.4 min, respectively. The retention times of the corresponding Re complexes on HPLC (UV detection) were 13.5, 18.4, 8.6, and 11.2 min, respectively.

In vitro binding experiments to evaluate the affinity of the ^{99m}Tc-labeled chalcones for Aβ aggregates were carried out in solutions (Figure 2). To make quantitative comparisons with ^{99m}Tc-BAT and ^{99m}Tc-MAMA, we showed the binding affinity as total Aβ(1−42) aggregate-bound radioactivity (%) at different concentrations of Aβ aggregates. In this assay, we also confirmed that the nonspecific Aβ(1−42) aggregate-bound radioactivity (%) was 1.9−3.2% in the four ^{99m}Tc-labeled chalcones, indicating that nearly all of the radioactivity occupied the specific binding site for Aβ aggregates. The percent radioactivity of the chalcones bound to aggregates increased dependent on the dose of Aβ(1−42). In terms of Aβ(1−42) aggregate-bound radioactivity, the derivatives ranked in the following

DOI: 10.1021/cn100042d | ACS Chem. Neurosci. (2010), 1, 598–607

Scheme 3. ^{99m}Tc Labeling of Chalcone Derivatives

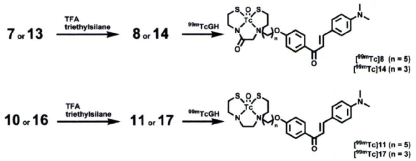

Table 1. HPLC Retention Times of ^{99m}Tc-Labeled Chalcones and Their Re Analogues and log *P* Values of ^{99m}Tc-Labeled Chalcones

^{99m}Tc compound	retention time (min)[a]	Re compound	retention time (min)[a]	log *P* of ^{99m}Tc compounds[b]
[^{99m}Tc]**8**	14.2	**9**	13.5	2.55 ± 0.19
[^{99m}Tc]**11**	20.3	**12**	18.4	2.73 ± 0.16
[^{99m}Tc]**14**	9.3	**15**	8.6	1.51 ± 0.09
[^{99m}Tc]**17**	12.4	**18**	11.2	2.51 ± 0.05

[a] Reversed-phase HPLC using a mixture of H_2O/acetonitrile (2/3) as a mobile phase. [b] The measurement was done in triplicate and repeated three times. Each value represents the mean ± SD for three independent experiments.

order: [^{99m}Tc]**11** > [^{99m}Tc]**8** > [^{99m}Tc]**14** > [^{99m}Tc]**17**. ^{99m}Tc complexes (^{99m}Tc-MAMA and ^{99m}Tc-BAT) showed no marked binding to Aβ(1−42) aggregates. This result suggests that the length of the alkyl chain between ^{99m}Tc complexes and the chalcone backbone played an important role in the binding of Aβ(1−42) aggregates, and the difference in ligand (MAMA and BAT) did not affect the affinity.

To confirm the affinity for β-amyloid plaques in the mouse brain, neuropathological fluorescent staining with Re-chalcone derivatives (**9**, **12**, **15**, and **18**) was carried out using Tg2576 mouse brain sections (Figure 3). Many β-amyloid plaques were clearly stained with the derivatives (Figure 3A,C,E,G), as reflected by the high affinity for Aβ aggregates in binding assays *in vitro*, while only minimum labeling was observed in the wild-type mouse brain (Figure 3I). The labeling pattern was consistent with that observed with thioflavin S (Figure 3B,D, F,H). These results suggest that the ^{99m}Tc-chalcones bind to β-amyloid plaques in the mouse brain in addition to having affinity for synthetic Aβ(1−42) aggregates.

Four ^{99m}Tc-labeled chalcones ([^{99m}Tc]**8**, [^{99m}Tc]**11**, [^{99m}Tc]**14**, [^{99m}Tc]**17**) were examined as to their biodistribution in normal mice (Table 2). A biodistribution study provides important information on brain uptake. The ideal β-amyloid imaging probe should have good blood−brain barrier penetration to deliver a sufficient dose into the brain while achieving rapid clearance from normal regions to result in a higher signal-to-noise ratio in the AD brain. Previous studies suggested that the

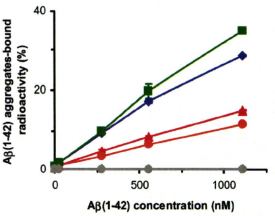

Figure 2. Binding assay of ^{99m}Tc-labeled chalcone derivatives (◆, blue) [^{99m}Tc]**8**, (■) [^{99m}Tc]**11**, (▲) [^{99m}Tc]**14**, (●, orange) [^{99m}Tc]**17**, (●, gray) ^{99m}Tc-MAMA, (◆, gray) ^{99m}Tc-BAT with Aβ(1−42) aggregates. Values are the mean ± standard error of the mean for three independent experiments.

optimal lipophilicity for entry into the brain is obtained with log *P* values of between 1 and 3 (*27*). All four ligands examined in the present study displayed optimal lipophilicity as reflected by their log *P* values (Table 1). Among the four ^{99m}Tc-labeled chalcones, [^{99m}Tc]**17** showed the highest uptake (1.48% ID/g at 2 min postinjection), but [^{99m}Tc]**8**, [^{99m}Tc]**11**, and [^{99m}Tc]**14** did not show sufficient uptake (0.32−0.78% ID/g at 2 min postinjection) despite their lipophilicity. The reason for the low uptake remains unknown. The uptake of [^{99m}Tc]**17** was greater than that of ^{99m}Tc-labeled Aβ imaging agents reported previously, supporting the feasibility of developing ^{99m}Tc-labeled probes for the detection of β-amyloid plaques *in vivo*. Thereafter, the radioactivity of [^{99m}Tc]**17** that accumulated in the brain was rapidly eliminated (0.17% ID/g at 60 min postinjection), a highly desirable property for imaging agents. The pharmacokinetics of [^{99m}Tc]**17** in the brain appears superior to that of any other ^{99m}Tc-labeled probe reported previously, indicating that this chalcone should be investigated further for the imaging of β-amyloid. [^{99m}Tc]**8**, [^{99m}Tc]**11**, and [^{99m}Tc]**14** showed no marked initial uptake, 0.32−0.78% ID/g, and were washed out from the brain relatively slowly (0.11−0.16% ID/g at 60 min). The uptake of [^{99m}Tc]**8**, [^{99m}Tc]**11**, and [^{99m}Tc]**14** appears insufficient for the imaging of β-amyloid plaques in the brain, and additional structural changes are needed to further improve the properties of these chalcone derivatives.

In conclusion, we successfully designed and synthesized novel chalcone derivatives conjugated with ^{99m}Tc or Re complexes for the detection of β-amyloid plaques in the brain. When *in vitro* plaque labeling was carried out using sections of brain from Tg2576 mice, four Re-chalcones intensely stained β-amyloid plaques. In addition, [^{99m}Tc]**17** displayed good uptake into and a rapid washout from the brain after its injection into normal mice. The combination of affinity for β-amyloid plaques, good uptake, and rapid

DOI: 10.1021/cn100042d | ACS Chem. Neurosci. (2010), 1, 598–607

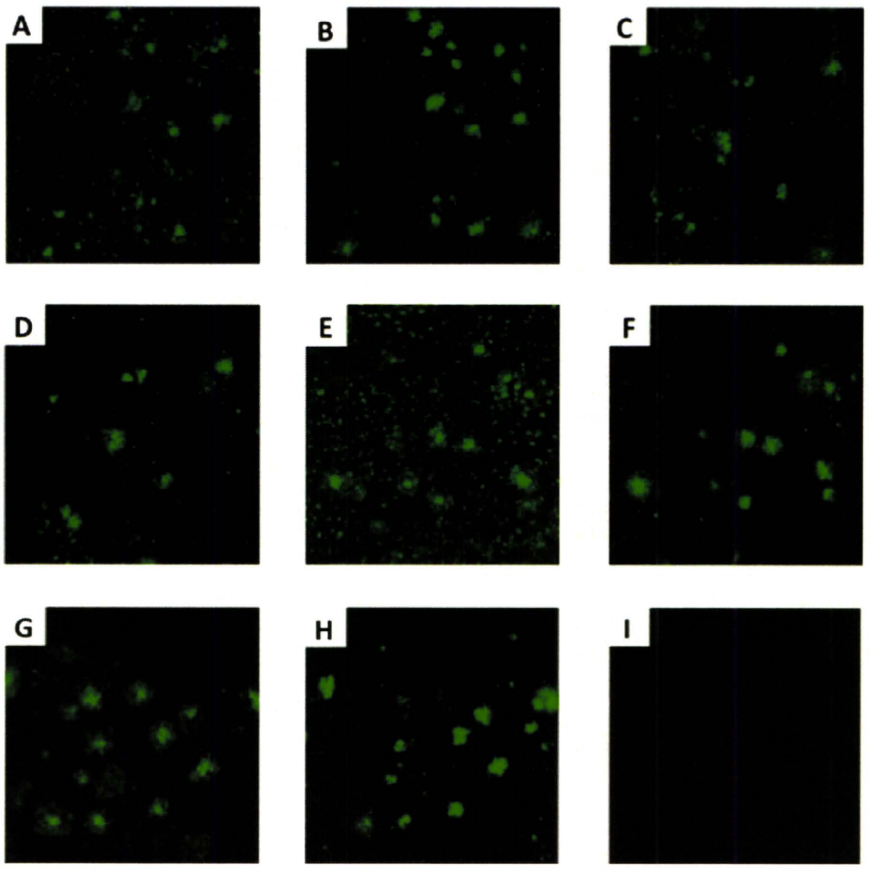

Figure 3. Fluorescent staining of chalcone derivatives **9** (A), **12** (C), **15** (E), and **18** (G) in 10-μm Tg2576 mouse brain sections. Labeled plaques were confirmed by staining of the adjacent sections with thioflavin-S (B, D, F, H). No apparent staining of **18** (I) was observed in the age-matched control mouse brain section.

clearance makes [^{99m}Tc]**17** a promising probe for the detection of β-amyloid plaques in the brain. The results of the present study should provide information useful to the development of ^{99m}Tc-labeled probes for the imaging of β-amyloid plaques in the brain.

Methods

General

All reagents were obtained commercially and used without further purification unless otherwise indicated. ^{1}H NMR spectra were obtained on a Varian Gemini 300 spectrometer with TMS as an internal standard. Coupling constants are reported in hertz. Multiplicity was defined by s (singlet), d (doublet), t (triplet), q (quartet), quin (quintet), and m (multiplet). Mass spectra were obtained on a JEOL IMS-DX. HPLC was performed with a Shimadzu system (a LC-10AT pump with a SPD-10A UV detector, λ = 254 nm) using a Cosmosil C18 column (Nakalai Tesque, 5C18-AR-II, 4.6 mm × 150 mm) and acetonitrile/H_2O (3/2) as the mobile phase at a flow rate of 1.0 mL/min. All key compounds were proven by this method to show >95% purity.

Chemistry

2-(Tritylthio)ethanamine Hydrochloride (1). A solution of 2-mercaptoethylamine hydrochloride (1.14 g, 10 mmol) and triphenylmethyl chloride (2.79 g, 10 mmol) in DMF (10 mL) was stirred at room temperature for 72 h. After the evaporation of DMF, the residue was redissolved in ethyl acetate and added to a 5% $NaHCO_3$ solution in an ice bath. The white precipitate that formed was filtered to yield **1** (3.50 g, 98% yield). ^{1}H NMR (300 MHz, $CDCl_3$) δ 2.31 (t, J = 6.8 Hz, 2H), 2.60 (t, J = 6.8 Hz, 2H), 7.18−7.31 (m, 9H), 7.43 (d, J = 7.2 Hz, 6H).

2-(2-(Tritylthio)ethylamino)-*N*-(2-(tritylthio)ethyl)acetamide (Tr-MAMA) (2). To a stirring solution of **1** (2.50 g, 7.02 mmol) in $CHCl_3$ (20 mL) and triethylamine (5 mL) was slowly added bromoacetyl bromide (0.5 mL, 5.76 mmol) in an ice bath, and the mixture was stirred at 0 °C for 3 h. The mixture was washed with a diluted H_2SO_4 (pH 3), a saturated $NaHCO_3$, and a saturated NaCl solution, sequentially. The organic layers were combined and dried with Na_2SO_4. Evaporation of the solvent gave a residue, which was purified by silica gel chromatography using $CHCl_3$ and then ethyl acetate to give 1.39 g of **2** (58% yield). ^{1}H NMR (300 MHz, $CDCl_3$) δ 2.35 (q, J = 6.6 Hz, 4H), 2.45 (t, J = 5.9 Hz, 2H), 3.02 (s, 2H), 3.07 (q, J = 6.3 Hz, 2H), 7.18−7.29 (m, 18H), 7.38−7.42 (m, 12H). MS m/z 679 (MH^+).

DOI: 10.1021/cn100042d | ACS Chem. Neurosci. (2010), 1, 598–607

Table 2. Biodistribution of Radioactivity after Injection of ^{99m}Tc-Labeled Chalcone Derivatives in Normal Mice[a]

organ	time after injection (min)			
	2	10	30	60
		[^{99m}Tc]**8**		
blood	1.85(0.31)	0.91(0.15)	0.62(0.16)	0.28(0.02)
liver	18.92(2.03)	24.48(1.34)	26.63(5.57)	17.05(1.52)
kidney	9.45(1.24)	7.62(3.79)	9.85(1.35)	5.25(0.87)
intestine[b]	4.71(0.63)	12.45(2.90)	34.90(3.01)	36.49(6.04)
spleen	4.16(0.52)	3.17(0.52)	2.37(0.48)	1.28(0.09)
lung	16.13(1.34)	6.59(1.23)	3.61(1.00)	1.44(0.17)
stomach[b]	0.76(0.10)	1.31(0.15)	2.06(0.65)	1.67(0.29)
pancreas	3.78(0.49)	5.28(0.33)	4.71(0.96)	2.27(0.14)
heart	11.05(1.99)	5.10(1.00)	2.16(0.63)	0.87(0.22)
brain	0.22(0.05)	0.32(0.14)	0.19(0.030)	0.11(0.01)
		[^{99m}Tc]**11**		
blood	2.49(0.24)	0.92(0.05)	0.50(0.11)	0.35(0.13)
liver	23.89(2.51)	24.03(4.51)	23.18(3.67)	21.95(4.58)
kidney	11.26(0.62)	9.66(0.58)	7.64(0.88)	6.39(1.51)
intestine[b]	6.27(0.31)	15.99(0.87)	37.18(2.54)	54.09(10.94)
spleen	3.15(0.22)	1.64(0.33)	0.69(0.16)	0.35(0.15)
lung	15.71(4.59)	4.54(0.57)	1.89(0.24)	1.28(0.49)
stomach[b]	0.95(0.14)	1.37(0.19)	1.77(0.62)	2.41(0.99)
pancreas	4.93(0.87)	3.94(0.84)	1.71(0.30)	0.80(0.32)
heart	13.17(1.42)	3.03(0.36)	1.30(0.35)	0.78(0.10)
brain	0.78(0.16)	0.55(0.06)	0.28(0.09)	0.16(0.09)
		[^{99m}Tc]**14**		
blood	7.84(2.85)	5.37(2.42)	1.55(0.62)	0.41(0.19)
liver	18.35(1.93)	24.89(2.27)	21.29(3.34)	12.96(3.14)
kidney	10.50(1.36)	11.03(2.66)	9.62(1.54)	4.65(0.75)
intestine[b]	3.70(0.55)	9.60(1.35)	31.67(4.85)	41.40(8.54)
spleen	5.87(2.07)	4.44(0.69)	2.71(0.92)	1.42(0.85)
lung	16.33(4.74)	7.87(1.60)	3.16(0.68)	4.12(4.25)
stomach[b]	0.85(0.21)	1.42(0.28)	2.29(0.61)	2.32(0.81)
pancreas	3.14(1.32)	5.30(2.14)	4.64(0.76)	1.63(0.37)
heart	13.26(2.46)	4.96(1.83)	2.54(0.56)	1.23(0.28)
brain	0.62(0.27)	0.47(0.13)	0.38(0.11)	0.16(0.08)
		[^{99m}Tc]**17**		
blood	2.81(0.76)	0.95(0.45)	0.56(0.30)	0.29(0.13)
liver	21.26(2.50)	27.33(2.45)	22.08(3.93)	14.34(0.60)
kidney	11.21(1.46)	8.54(0.64)	4.18(0.52)	1.92(0.41)
intestine[b]	6.22(0.40)	21.95(2.50)	42.24(3.78)	53.39(4.78)
spleen	2.91(0.61)	2.37(0.55)	0.74(0.16)	0.30(0.04)
lung	10.33(1.80)	5.92(1.38)	2.47(0.62)	0.73(0.27)
stomach[b]	1.14(0.26)	1.80(0.22)	1.93(0.19)	1.68(0.67)
pancreas	6.91(2.23)	4.45(0.54)	1.44(0.33)	0.47(0.06)
heart	11.71(2.13)	3.01(0.70)	0.98(0.26)	0.44(0.10)
brain	1.48(0.44)	1.09(0.20)	0.35(0.14)	0.17(0.06)

[a] Each value represents the mean (SD) for 3−6 mice at each interval. Expressed as % injected dose per gram. [b] Expressed as % injected dose per organ.

***tert*-Butyl-2-(2-(tritylthio)ethylamino)ethyl-2-(tritylthio)ethylcarbamate (Tr-BAT) (3).** To a solution of N^1,N^2-bis(2-(tritylthio)ethyl)ethane-1,2-diamine (3.33 g, 5 mmol) and DIPEA (0.86 mL, 5 mmol) in CH_2Cl_2 (80 mL) was added dropwise a solution of $(BOC)_2O$ (1.09 g, 5 mmol) in CH_2Cl_2 (20 mL) in an ice bath. The mixture was stirred at 0 °C for 1 h, concentrated, and purified by column chromatography ($CHCl_3/CH_3OH$ = 99:1) to give 3.59 g of **3** (94%). ^{1}H NMR (300 MHz, $CDCl_3$) δ 1.37 (s, 9H), 1.54 (s, broad, 1H), 2.46−2.28 (m, 8H), 2.96 (s, broad, 4H), 7.17−7.30 (m, 18H), 7.37−7.43 (m, 12H).

(*E*)-3-(4-(Dimethylamino)phenyl)-1-(4-hydroxyphenyl)prop-2-en-1-one (4). *p*-Hydroxyacetophenone (1.36 g, 10 mmol) and *p*-dimethylaminobenzaldehyde (1.49 g, 10 mmol) were dissolved in EtOH (15 mL). A 30-mL aliquot of a 10% aqueous KOH solution was then slowly added dropwise to the reaction mixture. The mixture was stirred for 12 h at 100 °C and then poured into a 1 M aqueous HCl solution and extracted with ethyl acetate. The organic layers were combined and dried over Na_2SO_4. Evaporation of the solvent afforded a residue, which was purified by silica gel chromatography ($CHCl_3/CH_3OH$ = 49:1) to give 1.86 g of **4** (70%). ^{1}H NMR (300 MHz, $CDCl_3$) δ 3.05 (s, 6H), 6.70 (d, J = 8.7 Hz, 2H), 6.91 (d, J = 9.0 Hz, 2H), 7.34 (d, J = 15.3 Hz, 1H), 7.55 (d, J = 9.0 Hz, 2H), 7.79 (d, J = 16.2 Hz, 1H), 7.99 (d, J = 9.0 Hz, 2H).

(*E*)-1-(4-(5-Bromopentyloxy)phenyl)-3-(4-(dimethylamino)-phenyl)prop-2-en-1-one (5). To a solution of **4** (1.51 g, 5.64 mmol) in acetonitrile (15 mL) were added 1,5-dibromopentane (1.54 mL, 11.4 mmol) and K_2CO_3 (1.5 g). The reaction mixture was heated to reflux for 4 h. After the acetonitrile was evaporated, the residue was poured into water and extracted with $CHCl_3$. The organic layer was combined and dried with Na_2SO_4. After the mixture was concentrated, the residue was redissolved in DMSO and washed using hexane. The DMSO layer was concentrated and purified by silica gel chromatography using $CHCl_3$ to give 1.48 g of **5** (63% yield). ^{1}H NMR (300 MHz, $CDCl_3$) δ 1.62−1.70 (m, 2H), 1.83−1.90 (m, 2H), 1.91−2.01 (m, 2H), 3.05 (s, 6H), 3.56 (t, J = 6.8 Hz, 2H), 4.06 (t, J = 6.3 Hz, 2H), 6.70 (d, J = 9.0 Hz, 2H), 6.95 (d, J = 8.7 Hz, 2H), 7.36 (d, J = 15.3 Hz, 1H), 7.55 (d, J = 8.7 Hz, 2H), 7.79 (d, J = 15.6 Hz, 1H), 8.02 (d, J = 9.0 Hz, 2H).

(*E*)-1-(4-(3-Bromopropoxy)phenyl)-3-(4-(dimethylamino)-phenyl)prop-2-en-1-one (6). To a solution of **4** (890 mg, 3.33 mmol) in acetonitrile (25 mL) were added 1,3-dibromopropane (0.679 mL, 6.66 mmol) and K_2CO_3 (1.0 g). The reaction mixture was heated to reflux for 4 h. After the acetonitrile was evaporated, the residue was poured into a saturated NaCl solution and extracted with $CHCl_3$. The organic layer was combined and dried with Na_2SO_4. After the mixture was concentrated, the residue was redissolved in DMF and washed using hexane. The DMF layer was concentrated and purified by silica gel chromatography ($CHCl_3/CH_3OH$ = 199:1) to give 981 mg of **6** (73% yield). ^{1}H NMR (300 MHz, $CDCl_3$) δ 2.35 (quin, J = 6.1 Hz, 2H), 3.04 (s, 6H), 3.61 (t, J = 6.5 Hz, 2H), 4.18 (t, J = 5.7 Hz, 2H), 6.69 (d, J = 9.0 Hz, 2H), 6.97 (d, J = 8.7 Hz, 2H), 7.35 (d, J = 15.3 Hz, 1H), 7.55 (d, J = 8.7 Hz, 2H), 7.79 (d, J = 15.6 Hz, 1H), 8.02 (d, J = 9.0 Hz, 2H).

Compound 7 (Tr-MAMA-C5-CH). To a solution of **5** (485 mg, 1.13 mmol) and **2** (830 mg, 1.22 mmol) in DMF (10 mL) was added DIPEA (1 mL). The reaction mixture was heated to reflux

DOI: 10.1021/cn100042d | ACS Chem. Neurosci. (2010), 1, 598–607

for 12 h. After the evaporation of the solvent, water was added. The mixture was extracted with $CHCl_3$. The organic layers were combined and dried with Na_2SO_4. Evaporation of the solvent gave a residue, which was purified by silica gel chromatography ($CHCl_3/CH_3OH$ = 199:1) to give 330 mg of **7** (29% yield). ^1H NMR (300 MHz, $CDCl_3$) δ 1.39 (s, 4H), 1.69−1.71 (m, 2H), 2.27−2.41 (m, 8H), 2.87 (s, 2H), 2.95−3.01 (m, 2H), 3.04 (s, 6H), 3.93 (t, J = 6.5 Hz, 2H), 6.70 (d, J = 9.0 Hz, 2H), 6.89 (d, J = 8.7 Hz, 2H), 7.14−7.27 (m, 18H), 7.32−7.39 (m, 13H), 7.55 (d, J = 9.0 Hz, 2H), 7.79 (d, J = 15.6 Hz, 1H), 7.99 (d, J = 9.0 Hz, 2H). MS m/z 1014 (MH^+).

Compound 8 (MAMA-C5-CH). To a solution of a little **7** in TFA (200 mL) was added triethylsilane (10 mL), and the solution was mixed. The solvent was removed under a stream of nitrogen gas to give **8**. MS m/z 530 (MH^+).

Compound 9 (Re-MAMA-C5-CH). To a solution of **7** (82 mg, 0.081 mmol) in TFA (4 mL) was added triethylsilane (0.2 mL), and the solution was mixed, and then the solvent was removed under a stream of nitrogen gas. The residue was resolved in a mixed solvent (22 mL, CH_2Cl_2/CH_3OH = 10:1), to which were added $(Ph_3P)_2ReOCl_3$ (135 mg, 0.162 mmol) and 1 M sodium acetate in methanol (4 mL). The reaction mixture was heated to reflux for 6 h and, after cooling to room temperature, mixed with ethyl acetate (60 mL) and filtered. Evaporation of the solvent gave a residue, which was purified by silica gel chromatography ($CHCl_3/CH_3OH$ = 49:1) and then RP-HPLC (acetonitrile/H_2O = 4:1) to give 20 mg (35%) of **9**. ^1H NMR (300 MHz, $CDCl_3$) δ 1.60−1.67 (m, 2H), 1.89−1.92 (m, 4H), 2.82−2.91 (m, 1H), 3.05 (s, 6H), 3.14−3.27 (m, 3H), 3.33−3.42 (m, 1H), 3.52−3.65 (m, 1H), 3.95−4.16 (m, 6H), 4.56−4.62 (m, 1H), 4.67 (d, J = 16.5 Hz, 1H), 6.70 (d, J = 8.7 Hz, 2H), 6.95 (d, J = 8.7 Hz, 2H), 7.35 (d, J = 15.6 Hz, 1H), 7.55 (d, J = 9.0 Hz, 2H), 7.79 (d, J = 15.6 Hz, 1H), 8.03 (d, J = 8.7 Hz, 2H). HRMS m/z $C_{28}H_{37}N_3O_4ReS_2$ found 730.1748, calcd 730.1783 (MH^+).

Compound 10 (Tr-BAT-C5-CH). To a solution of **5** (630 mg, 1.51 mmol) and **3** (855 mg, 1.12 mmol) in DMF (20 mL) was added DIPEA (2 mL). The reaction mixture was heated to reflux for 12 h. After the evaporation of the solvent, the residue was purified by silica gel chromatography using $CHCl_3$ and then ethyl acetate/hexane (1:2) to give 126 mg of **10** (10% yield). ^1H NMR (300 MHz, $CDCl_3$) δ 1.32−1.37 (m, 12H), 1.70−1.77 (m, 2H), 2.20−2.35 (m, 10H), 2.85−3.01 (m, 4H), 3.04 (s, 6H), 3.98 (t, J = 6.5 Hz, 2H), 6.69 (d, J = 9.3 Hz, 2H), 6.93 (d, J = 8.7 Hz, 2H), 7.15−7.29 (m, 18H), 7.33−7.42 (m, 13H), 7.55 (d, J = 8.7 Hz, 2H), 7.79 (d, J = 15.6 Hz, 1H), 8.01 (d, J = 9.0 Hz, 2H). MS m/z 1100 (MH^+).

Compound 11 (BAT-C5-CH). To a solution of **10** in TFA (200 mL) was added triethylsilane (10 mL), and the solution was mixed. The solvent was removed under a stream of nitrogen gas to give **11**. MS m/z 516 (MH^+).

Compound 12 (Re-BAT-C5-CH). To a solution of **10** (110 mg, 0.100 mmol) in TFA (4 mL) was added triethylsilane (0.2 mL), and the solution was mixed, and then the solvent was removed under a stream of nitrogen gas. The residue was resolved in a mixed solvent (22 mL, CH_2Cl_2/CH_3OH = 10:1), to which were added $(Ph_3P)_2ReOCl_3$ (167 mg, 0.200 mmol) and 1 M sodium acetate in methanol (4 mL). The reaction mixture was heated to reflux for 6 h and, after cooling to room temperature, mixed with ethyl acetate (60 mL) and filtered. Evaporation of the solvent gave a residue, which was purified by silica gel chromatography ($CHCl_3/CH_3OH$ = 49:1) and then RP-HPLC (acetonitorile/H_2O = 4:1) to give 44 mg (61%) of **12**. ^1H NMR (300 MHz, $CDCl_3$) δ 1.60−1.73 (m, 2H), 1.87−1.92 (m, 4H), 2.72−2.78 (m, 1H), 2.96−3.00 (m, 2H), 3.05 (s, 6H), 3.21−3.41 (m, 4H), 3.53−3.63 (m, 1H), 3.76−3.92 (m, 3H), 4.06−4.17 (m, 5H), 6.70 (d, J = 8.7 Hz, 2H), 6.96 (d, J = 9.0 Hz, 2H), 7.36 (d, J = 15.6 Hz, 1H), 7.56 (d, J = 9.0 Hz, 2H), 7.79 (d, J = 15.6 Hz, 1H), 8.03 (d, J = 9.0 Hz, 2H). HRMS m/z $C_{28}H_{39}N_3O_3ReS_2$ found 716.1990, calcd 716.1990 (MH^+).

Compound 13 (Tr-MAMA-C3-CH). To a solution of **6** (981 mg, 2.53 mmol) and **2** (1.72 g, 2.53 mmol) in DMF (30 mL) was added DIPEA (3 mL). The reaction mixture was heated to reflux for 12 h. After the evaporation of the solvent, water was added. The mixture was extracted with $CHCl_3$. The organic layers were combined and dried with Na_2SO_4. Evaporation of the solvent gave a residue, which was purified by silica gel chromatography (ethyl acetate/hexane = 3:2) to give 714 mg of **13** (29% yield). ^1H NMR (300 MHz, $CDCl_3$) δ 1.80−1.87 (m, 2H), 2.28 (t, J = 6.3 Hz, 2H), 2.33−2.43 (m, 4H), 2.51 (t, J = 6.9 Hz, 2H), 2.91 (s, 2H), 2.99−3.03 (m, 2H), 3.05 (s, 6H), 3.99 (t, J = 5.9 Hz, 2H), 6.70 (d, J = 9.0 Hz, 2H), 6.86 (d, J = 9.0 Hz, 2H), 7.14−7.27 (m, 18H), 7.29−7.38 (m, 13H), 7.54 (d, J = 8.7 Hz, 2H), 7.78 (d, J = 15.3 Hz, 1H), 7.93 (d, J = 9.0 Hz, 2H). MS m/z 986 (MH^+).

Compound 14 (MAMA-C3-CH). To a solution of **13** in TFA (200 mL) was added triethylsilane (10 mL), and the solution was mixed. The solvent was removed under a stream of nitrogen gas to give **14**. MS m/z 502 (MH^+).

Compound 15 (Re-MAMA-C3-CH). To a solution of **13** (99 mg, 0.100 mmol) in TFA (4 mL) was added triethylsilane (0.2 mL), and the solution was mixed, and then the solvent was removed under a stream of nitrogen gas. The residue was resolved in a mixed solvent (22 mL, CH_2Cl_2/CH_3OH = 10:1), to which were added $(Ph_3P)_2ReOCl_3$ (167 mg, 0.200 mmol) and 1 M sodium acetate in methanol (4 mL). The reaction mixture was heated to reflux for 6 h and, after cooling to room temperature, mixed with ethyl acetate (60 mL) and filtered. Evaporation of the solvent gave a residue, which was purified with silica gel chromatography ($CHCl_3/CH_3OH$ = 49:1) and then RP-HPLC (acetonitorile/H_2O = 4:1) to give 20 mg (29%) of **15**. ^1H NMR (300 MHz, $CDCl_3$) δ 1.65−1.75 (m, 1H), 2.32−2.37 (m, 2H), 2.90−2.98 (m, 1H), 3.05 (s, 6H), 3.15−3.34 (m, 3H), 3.40−3.52 (m, 1H), 3.81−3.86 (m, 1H), 4.09−4.19 (m, 5H), 4.58−4.64 (m, 1H), 4.74 (d, J = 16.2 Hz, 1H), 6.70 (d, J = 9.0 Hz, 2H), 6.96 (d, J = 8.7 Hz, 2H), 7.40 (d, J = 15.3 Hz, 1H), 7.56 (d, J = 8.7 Hz, 2H), 7.79 (d, J = 15.3 Hz, 1H), 8.03 (d, J = 9.0 Hz, 2H). HRMS m/z $C_{26}H_{33}N_3O_4ReS_2$ found 702.1476, calcd 702.1470 (MH^+).

Compound 16 (Tr-BAT-C3-CH). To a solution of **6** (243 mg, 0.626 mmol) and **3** (479 mg, 0.626 mmol) in DMF (10 mL) was added DIPEA (1 mL). The reaction mixture was heated to reflux for 12 h. After the evaporation of the solvent, a saturated NaCl solution was added. The mixture was extracted with $CHCl_3$. The organic layers were combined and dried with Na_2SO_4. Evaporation of the solvent gave a residue, which was purified by silica gel chromatography

DOI: 10.1021/cn100042d | ACS Chem. Neurosci. (2010), 1, 598–607

using $CHCl_3$ and then ethyl acetate/hexane (1:2) to give 128 mg of **16** (19% yield). ^{1}H NMR (300 MHz, $CDCl_3$) δ 1.37 (s, 9H), 1.73 (t, J = 6.0 Hz, 2H), 2.24−2.38 (m, 10H), 2.88−2.95 (m, 4H), 3.04 (s, 6H), 3.97 (t, J = 6.2 Hz, 2H), 6.70 (d, J = 9.0 Hz, 2H), 6.89 (d, J = 8.7 Hz, 2H), 7.15−7.31 (m, 19H), 7.37−7.41 (m, 12H), 7.54 (d, J = 9.0 Hz, 2H), 7.78 (d, J = 15.6 Hz, 1H), 7.96 (d, J = 8.7 Hz, 2H). MS m/z 1072 (MH^+).

Compound 17 (BAT-C3-CH). To a solution of **16** in TFA (200 mL) was added triethylsilane (10 mL), and the solution was mixed. The solvent was removed under a stream of nitrogen gas to give **17**. MS m/z 488 (MH^+).

Compound 18 (Re-BAT-C3-CH). To a solution of **16** (104 mg, 0.097 mmol) in TFA (4 mL) was added triethylsilane (0.2 mL), and the solution was mixed, and then the solvent was removed under a stream of nitrogen gas. The residue was resolved in a mixed solvent (22 mL, CH_2Cl_2/CH_3OH = 10:1), to which were added $(Ph_3P)_2ReOCl_3$ (167 mg, 0.200 mmol) and 1 M sodium acetate in methanol (4 mL). The reaction mixture was heated to reflux for 6 h and, after cooling to room temperature, mixed with ethyl acetate (60 mL) and filtered. Evaporation of the solvent gave a residue, which was purified with silica gel chromatography ($CHCl_3/CH_3OH$ = 49:1) and then RP-HPLC (acetonitrile/H_2O = 4:1) to give 44 mg (66%) of **18**. ^{1}H NMR (300 MHz, $CDCl_3$) δ1.75−1.85 (m, 1H), 2.31−2.38 (m, 2H), 2.76−2.82 (m, 1H), 2.91−3.08 (m, 2H), 3.05 (s, 6H), 3.24−3.49 (m, 4H), 3.76−4.00 (m, 3H), 4.12−4.33 (m, 5H), 6.70 (d, J = 9.0 Hz, 2H), 6.95 (d, J = 9.0 Hz, 2H), 7.35 (d, J = 15.3 Hz, 1H), 7.56 (d, J = 9.0 Hz, 2H), 7.79 (d, J = 15.3 Hz, 1H), 8.03 (d, J = 8.7 Hz, 2H). HRMS m/z $C_{26}H_{35}N_3O_3ReS_2$ found 688.1631, calcd 688.1677 (MH^+).

^{99m}Tc Labeling Reaction

To a solution of sodium heptonate dehydrate (2.0 g, 7.04 mmol) in nanopure water (25 mL) was added a 0.75 mL aliquot of a $SnCl_2 \cdot 2H_2O$ solution [12 mg of Tin(II) chloride dehydrate (53.2 mmol) was dissolved in 0.1 M HCl (15 μL)]. This solution was adjusted to pH 8.5−9.0 with a small amount of 0.1 M NaOH and then lyophilized to give tin glucoheptonate (SnGH) kit. SnGH kit (1 mg) was added to a $Na^{99m}TcO_4$ solution (200 μL) and reacted at room temperature for 10 min to give a ^{99m}TcGH solution. To solutions of **7**, **10**, **13**, and **16** (0.5 mg) in TFA (200 μL) was added triethylsilane (10 μL), and the solutions were mixed, and then the solvents were removed under a stream of nitrogen gas. The residues were resolved in acetonitrile (200 μL), to which were added a 0.1 M HCl solution (15 μL) and the ^{99m}TcGH solution (200 mL). The reaction mixtures were heated to 80−90 °C for 10 min. The residue taken up in 100 μL of acetonitrile was purified by a reversed-phase HPLC system with an isocratic solvent of acetonitrile/H_2O (3/2) as the mobile phase at a flow rate of 1.0 mL/min. After cooling to room temperature, the mixtures were purified with RP-HPLC to give [^{99m}Tc]**8**, [^{99m}Tc]**11**, [^{99m}Tc]**14**, and [^{99m}Tc]**17**. The desired fraction was collected in a flask and evaporated dry. The radiochemical identity of [^{99m}Tc]**8**, [^{99m}Tc]**11**, [^{99m}Tc]**14**, and [^{99m}Tc]**17** was verified with the corresponding Re-complex from the HPLC profiles. The final ^{99m}Tc-complexes showed a single peak of radioactivity at retention times of 14.2, 20.3, 9.3, and 12.4 min, respectively, close to those of the Re complexes. The four ^{99m}Tc-complexes were obtained in 46−95% radiochemical yields with a radiochemical purity of >95% after HPLC.

Partition Coefficient

Partition coefficients were measured by mixing the [^{99m}Tc]tracer with 3 mL each of 1-octanol and buffer (0.1 M phosphate, pH 7.4) in a test tube. The test tube was vortexed for 3 min at room temperature, then centrifuged for 5 min. Two weighed samples (0.5 mL) from the 1-octanol and buffer layers were measured in a well counter. The partition coefficient was determined by calculating the ratio of counts per minute per gram of 1-octanol to that of buffer. Samples from the 1-octanol layer were repartitioned until consistent partitions of coefficient values were obtained. The measurement was done in triplicate and repeated three times.

Binding Assays Using the Aggregated Aβ Peptides in Solution

A solid form of Aβ(1−42) was purchased from Peptide Institute (Osaka, Japan). Aggregation was carried out by gently dissolving the peptide (0.25 mg/mL) in a buffer solution (pH 7.4) containing 10 mM sodium phosphate and 1 mM EDTA. The solutions were incubated at 37 °C for 42 h with gentle and constant shaking. The binding assay was performed by mixing 50 μL of Aβ(1−42) aggregates (0−100 μg/mL), 50 μL of an appropriate concentration of the ^{99m}Tc-labeled form ([^{99m}Tc]**8**, [^{99m}Tc]**11**, [^{99m}Tc]**14**, [^{99m}Tc]**17**), and 900 μL of 30% ethanol in 12 mm × 75 mm borosilicate glass tubes. Nonspecific binding was defined in the presence of 1 μM of chalcone derivative (4-dimethylamino-4′-iodo-chalcone) (*20*). After incubation for 3 h at room temperature, the mixture was filtered through GF/B filters (Whatman, Kent, U.K.) using an M-24 cell harvester (Brandel, Gaithersburg, MD). Filters containing the bound ^{99m}Tc-labeled form were examined in a γ counter (Perkin-Elmer, WIZARD^2 2470).

Biodistribution in Normal Mice

The experiments with animals were conducted in accordance with our institutional guidelines and approved by the Nagasaki University Animal Care Committee. A saline solution (100 μL) of ^{99m}Tc-chalcones (1.0×10^7 cpm/mL) containing ethanol (30 μL) was injected intravenously directly into the tail of ddY mice (5 weeks old, 22−25 g). The mice were sacrificed at various time points postinjection. The organs of interest were removed and weighed, and radioactivity was measured with an automatic γ counter (Perkin-Elmer, WIZARD^2 2470).

Neuropathological Staining of Mouse Brain Sections

The Tg2576 transgenic (female, 30-month-old) and wild-type mice (female, 30-month-old) mice were used as the Alzheimer's model and control, respectively. After the mice were sacrificed by decapitation, the brains were immediately removed and frozen in powdered dry ice. The frozen blocks were sliced into serial sections, 10 μm thick. Each slide was incubated with a 50% EtOH solution (2.5−10 μM) of **9**, **12**, **15**, and **18** for 2−9 h. The sections were washed in 50% EtOH for 5 min two times and examined for **9**, **12**, **15**, and **18** with excitation of 458 nm using a microscope (Carl Zeiss, LSM710). Thereafter, the serial sections were also stained with thioflavin S, a pathological dye commonly used for staining β-amyloid plaques in the brain.

DOI: 10.1021/cn100042d | ACS Chem. Neurosci. (2010), 1, 598–607

Author Information

Corresponding Author

*For M. Ono: phone +81-75-753-4608, fax +81-75-753-4568, e-mail ono@pharm.kyoto-u.ac.jp. For M. Nakayama: phone +81-95-819-2441, fax +81-95-819-2441, e-mail morio@nagasaki-u.ac.jp.

Funding Sources

This study was supported by the Program for Promotion of Fundamental Studies in Health Sciences of the National Institute of Biomedical Innovation (NIBIO), a Health Labour Sciences Research Grant, and a Grant-in-aid for Young Scientists (A) and Exploratory Research from the Ministry of Education, Culture, Sports, Science and Technology, Japan.

References

1. Selkoe, D. J. (2001) Alzheimer's disease: Genes, proteins, and therapy. *Physiol. Rev. 81*, 741–766.

2. Selkoe, D. J. (2000) Imaging Alzheimer's amyloid. *Nat. Biotechnol. 18*, 823–824.

3. Mathis, C. A., Wang, Y., and Klunk, W. E. (2004) Imaging β-amyloid plaques and neurofibrillary tangles in the aging human brain. *Curr. Pharm. Des. 10*, 1469–1492.

4. Nordberg, A. (2004) PET imaging of amyloid in Alzheimer's disease. *Lancet Neurol. 3*, 519–527.

5. Mathis, C. A., Wang, Y., Holt, D. P., Huang, G. F., Debnath, M. L., and Klunk, W. E. (2003) Synthesis and evaluation of ^{11}C-labeled 6-substituted 2-arylbenzothiazoles as amyloid imaging agents. *J. Med. Chem. 46*, 2740–2754.

6. Klunk, W. E., Engler, H., Nordberg, A., Wang, Y., Blomqvist, G., Holt, D. P., Bergstrom, M., Savitcheva, I., Huang, G. F., Estrada, S., Ausen, B., Debnath, M. L., Barletta, J., Price, J. C., Sandell, J., Lopresti, B. J., Wall, A., Koivisto, P., Antoni, G., Mathis, C. A., and Langstrom, B. (2004) Imaging brain amyloid in Alzheimer's disease with Pittsburgh Compound-B. *Ann. Neurol. 55*, 306–319.

7. Ono, M., Wilson, A., Nobrega, J., Westaway, D., Verhoeff, P., Zhuang, Z. P., Kung, M. P., and Kung, H. F. (2003) ^{11}C-Labeled stilbene derivatives as Aβ-aggregate-specific PET imaging agents for Alzheimer's disease. *Nucl. Med. Biol. 30*, 565–571.

8. Verhoeff, N. P., Wilson, A. A., Takeshita, S., Trop, L., Hussey, D., Singh, K., Kung, H. F., Kung, M. P., and Houle, S. (2004) In-vivo imaging of Alzheimer disease β-amyloid with [^{11}C]SB-13 PET. *Am. J. Geriatr. Psychiatry 12*, 584–595.

9. Zhang, W., Oya, S., Kung, M. P., Hou, C., Maier, D. L., and Kung, H. F. (2005) F-18 polyethyleneglycol stilbenes as PET imaging agents targeting Aβ aggregates in the brain. *Nucl. Med. Biol. 32*, 799–809.

10. Rowe, C. C., Ackerman, U., Browne, W., Mulligan, R., Pike, K. L., O'Keefe, G., Tochon-Danguy, H., Chan, G., Berlangieri, S. U., Jones, G., Dickinson-Rowe, K. L., Kung, H. P., Zhang, W., Kung, M. P., Skovronsky, D., Dyrks, T., Holl, G., Krause, S., Friebe, M., Lehman, L., Lindemann, S., Dinkelborg, L. M., Masters, C. L., and Villemagne, V. L. (2008) Imaging of amyloid β in Alzheimer's disease with ^{18}F-BAY94-9172, a novel PET tracer: proof of mechanism. *Lancet Neurol. 7*, 129–135.

11. Kudo, Y., Okamura, N., Furumoto, S., Tashiro, M., Furukawa, K., Maruyama, M., Itoh, M., Iwata, R., Yanai, K., and Arai, H. (2007) 2-(2-[2-Dimethylaminothiazol-5-yl]ethenyl)-6-(2-[fluoro]ethoxy)benzoxazole: A novel PET agent for *in vivo* detection of dense amyloid plaques in Alzheimer's disease patients. *J. Nucl. Med. 48*, 553–561.

12. Agdeppa, E. D., Kepe, V., Liu, J., Flores-Torres, S., Satyamurthy, N., Petric, A., Cole, G. M., Small, G. W., Huang, S. C., and Barrio, J. R. (2001) Binding characteristics of radiofluorinated 6-dialkylamino-2-naphthylethylidene derivatives as positron emission tomography imaging probes for β-amyloid plaques in Alzheimer's disease. *J. Neurosci. 21*, No. RC189.

13. Shoghi-Jadid, K., Small, G. W., Agdeppa, E. D., Kepe, V., Ercoli, L. M., Siddarth, P., Read, S., Satyamurthy, N., Petric, A., Huang, S. C., and Barrio, J. R. (2002) Localization of neurofibrillary tangles and β-amyloid plaques in the brains of living patients with Alzheimer disease. *Am. J. Geriatr. Psychiatry 10*, 24–35.

14. Kung, M. P., Hou, C., Zhuang, Z. P., Zhang, B., Skovronsky, D., Trojanowski, J. Q., Lee, V. M., and Kung, H. F. (2002) IMPY: An improved thioflavin-T derivative for *in vivo* labeling of β-amyloid plaques. *Brain Res. 956*, 202–210.

15. Zhuang, Z. P., Kung, M. P., Wilson, A., Lee, C. W., Plossl, K., Hou, C., Holtzman, D. M., and Kung, H. F. (2003) Structure–activity relationship of imidazo[1,2-*a*]pyridines as ligands for detecting β-amyloid plaques in the brain. *J. Med. Chem. 46*, 237–243.

16. Newberg, A. B., Wintering, N. A., Clark, C. M., Plossl, K., Skovronsky, D., Seibyl, J. P., Kung, M. P., and Kung, H. F. (2006) Use of ^{123}I IMPY SPECT to differentiate Alzheimer's disease from controls. *J. Nucl. Med. 47*, 78P.

17. Zhang, W., Kung, M. P., Oya, S., Hou, C., and Kung, H. F. (2007) ^{18}F-labeled styrylpyridines as PET agents for amyloid plaque imaging. *Nucl. Med. Biol. 34*, 89–97.

18. Choi, S. R., Golding, G., Zhuang, Z., Zhang, W., Lim, N., Hefti, F., Benedum, T. E., Kilbourn, M. R., Skovronsky, D., and Kung, H. F. (2009) Preclinical properties of ^{18}F-AV-45: A PET agent for Aβ plaques in the brain. *J. Nucl. Med. 50*, 1887–1894.

19. Ono, M., Haratake, M., Mori, H., and Nakayama, M. (2007) Novel chalcones as probes for *in vivo* imaging of β-amyloid plaques in Alzheimer's brains. *Bioorg. Med. Chem. 15*, 6802–6809.

20. Ono, M., Hori, M., Haratake, M., Tomiyama, T., Mori, H., and Nakayama, M. (2007) Structure-activity relationship of chalcones and related derivatives as ligands for detecting of β-amyloid plaques in the brain. *Bioorg. Med. Chem. 15*, 6388–6396.

21. Ono, M., Watanabe, R., Kawashima, H., Cheng, Y., Kimura, H., Watanabe, H., Haratake, M., Saji, H., and Nakayama, M. (2009) Fluoro-pegylated chalcones as positron emission tomography probes for *in vivo* imaging of β-amyloid plaques in Alzheimer's disease. *J. Med. Chem. 52*, 6394–6401.

22. Han, H., Cho, C. G., and Lansbury, P. T., Jr. (1996) Technetium complexes for the quantitation of brain amyloid. *J. Am. Chem. Soc. 118*, 4506–4507.

23. Dezutter, N. A., Dom, R. J., de Groot, T. J., Bormans, G. M., and Verbruggen, A. M. (1999) ^{99m}Tc-MAMA-chrysamine G, a probe for β-amyloid protein of Alzheimer's disease. *Eur. J. Nucl. Med. 26*, 1392–1399.

24. Chen, X., Yu, P., Zhang, L., and Liu, B. (2008) Synthesis and biological evaluation of ^{99m}Tc, Re-monoamine-monoamide conjugated to 2-(4-aminophenyl)benzothiazole as potential probes for β-amyloid plaques in the brain. *Bioorg. Med. Chem. Lett. 18*, 1442–1445.

25. Serdons, K., Verduyckt, T., Cleynhens, J., Terwinghe, C., Mortelmans, L., Bormans, G., and Verbruggen, A. (2007) Synthesis and evaluation of a ^{99m}Tc-BAT-phenylbenzothiazole conjugate as a potential *in vivo* tracer for visualization of amyloid β. *Bioorg. Med. Chem. Lett. 17*, 6086–6090.

26. Oya, S., Plossl, K., Kung, M. P., Stevenson, D. A., and Kung, H. F. (1998) Small and neutral Tc(v)O BAT, bisaminoethanethiol (N2S2) complexes for developing new brain imaging agents. *Nucl. Med. Biol. 25*, 135–140.

27. Dishino, D. D., Welch, M. J., Kilbourn, M. R., and Raichle, M. E. (1983) Relationship between lipophilicity and brain extraction of C-11-labeled radiopharmaceuticals. *J. Nucl. Med. 24*, 1030–1038.

Note Added after ASAP Publication

This paper was published on the Web on July 8, 2010, with an error in Figure 3. The corrected version was reposted on July 13, 2010.

DOI: 10.1021/cn100042d | *ACS Chem. Neurosci.* (2010), *1*, 598–607

ACS Medicinal Chemistry Letters

pubs.acs.org/acsmedchemlett

Fluorinated Benzofuran Derivatives for PET Imaging of β-Amyloid Plaques in Alzheimer's Disease Brains

Yan Cheng,[†] Masahiro Ono,*[,†] Hiroyuki Kimura,[†] Shinya Kagawa,[‡] Ryuichi Nishii,[‡] Hidekazu Kawashima,[†] and Hideo Saji*[,†]

[†]Department of Patho-Functional Bioanalysis, Graduate School of Pharmaceutical Sciences, Kyoto University, Yoshida Shimoadachi-cho, Sakyo-ku, Kyoto 606-8501, Japan, and [‡]Shiga Medical Center Research Institute, 5-4-30, Moriyama, Moriyama City, Shiga, 524-8524, Japan

ABSTRACT A series of fluorinated benzofuran derivatives as potential tracers for positron emission tomography (PET) targeting β-amyloid plaques in the brains of patients with Alzheimer's disease (AD) were synthesized and evaluated. The derivatives were produced using an intramolecular Wittig reaction. In experiments in vitro, all displayed high affinity for Aβ(1−42) aggregates with K_i values in the nanomolar range. Radiofluorinated **17**, [^{18}F]**17**, in particular labeled β-amyloid plaques in sections of Tg2576 mouse brain and displayed high uptake (5.66% ID/g) at 10 min postinjection, sufficient for PET imaging. In addition, in vivo β-amyloid plaque labeling can be clearly demonstrated with [^{18}F]**17** in Tg2576 mice. In conclusion, [^{18}F]**17** may be useful for detecting β-amyloid plaques in patients with AD.

KEYWORDS Alzheimer's disease, fluorine-18, benzofuran, positron emission tomography (PET)

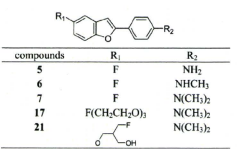

compounds	R_1	R_2
5	F	NH_2
6	F	$NHCH_3$
7	F	$N(CH_3)_2$
17	$F(CH_2CH_2O)_3$	$N(CH_3)_2$
21		$N(CH_3)_2$

Alzheimer's disease (AD) is a neurodegenerative disorder characterized by dementia, cognitive impairment, and memory loss. Autopsied brains of AD patients show neuropathological features such as the presence of senile plaques and neurofibrillary tangles, which contain β-amyloid peptides (Aβ) and highly phosphorylated τ proteins. Aβ aggregates in the brain are a hallmark of AD.[1,2] The quantitative evaluation of Aβ aggregates in the brain with noninvasive techniques such as positron emission tomography (PET) and single photon emission computed tomography (SPECT) would allow a presymptomatic diagnosis and the monitoring of putative effects of neuroprotective treatments. Thus, great efforts have been made to develop radiotracers that bind to β-amyloid plaques in vivo.[3−5]

Recent success in developing radiolabeled agents targeting Aβ aggregates has provided a window of opportunity to improve the diagnosis of AD. Preliminary reports of PET imaging suggested that [^{11}C]4-*N*-methylamino-4′-hydroxystilbene (SB-13),[6] [^{11}C]2-(4′-(methylaminophenyl)-6-hydroxybenzothiazole (PIB),[7,8] and [^{11}C]2-(2-[2-dimethylaminothiazol-5-yl]ethenyl)-6-(2-[fluoro]ethoxy)benzoxazole (BF-227)[9] showed differential uptake and retention in the brain of AD patients as compared to controls. However, ^{11}C is a positron-emitting isotope with a short $t_{1/2}$ (20 min), which limits its clinical application. Recent efforts have focused on the development of comparable agents labeled with a longer half-life isotope, ^{18}F ($t_{1/2}$, 110 min). Preliminary studies with [^{18}F]-2-(1-(2-(*N*-(2-fluoroethyl)-*N*-methylamino)-naphthalene-6-yl)ethylidene)malononitrile ([^{18}F]FDDNP)[10,11] showed differential uptake and retention in the brain of AD patients for the first time. More recently, a stilbene derivative, [^{18}F]BAY94-9172,[12,13] and a styrylpyridine derivative, [^{18}F]AV-45,[14,15] and a fluorinated PIB analogue, [^{18}F]GE-067,[16] have proven useful in the imaging of β-amyloid plaques in living human brain tissue in clinical trials (Figure 1).

To search for more candidates for ^{18}F-labeled tracers for PET, we planned to evaluate a new series of benzofuran derivatives previously reported as useful radioiodinated or ^{11}C-labeled probes for imaging β-amyloid plaques.[17,18] The derivatives showed good affinity for Aβ aggregates in vitro in binding experiments using synthetic Aβ aggregates and neuropathological staining of AD brain sections. We report here the in vitro and in vivo evaluation of a series of fluorinated benzofuran derivatives as probes for imaging β-amyloid plaques by PET.

The synthesis of the fluorinated benzofuran derivatives is outlined in Schemes 1−3. The key step in the formation of the benzofuran backbone is accomplished by an intramolecular Wittig reaction between triphenyl phosphonium salt and 4-nitrobenzoyl chloride or 4-dimethylaminobenzoyl chloride.[17] The desired Wittig reagent, **3**, was readily prepared from 5-fluoro-2-hydroxybenzyl alcohol and triphenylphosphine hydrobromide (yield 71%). Another Wittig reagent, **13**, was readily prepared from 2-hydroxy-5-methoxybenzyl alcohol and triphenylphosphine hydrobromide (yield 84%). Wittig reactions afforded the desired benzofurans (**4**, **7**, and **14**) in yields of 31, 55, and 27%, respectively.

Received Date: April 19, 2010
Accepted Date: June 30, 2010
Published on Web Date: July 11, 2010

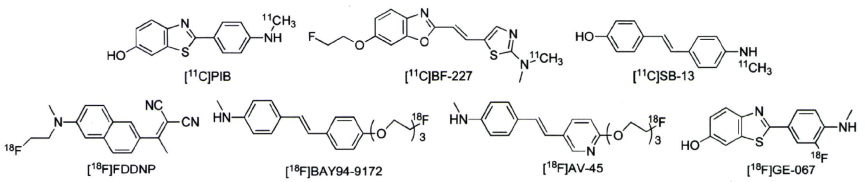

Figure 1. Chemical structures of PET imaging agents targeting β-amyloid plaques in AD patients.

Scheme 1[a]

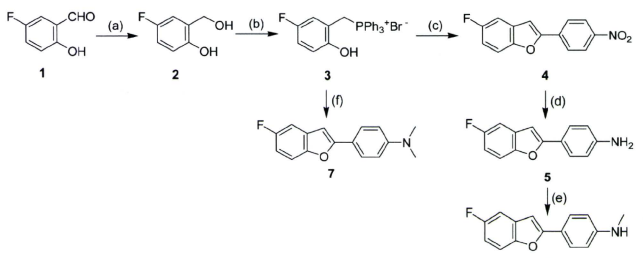

[a] Reagents and conditions: (a) $NaBH_4$, ethanol. (b) Triphenylphosphine hydrobromide, acetonitrile, reflux. (c) 4-Nitrobenzoyl chloride, toluene/NEt_3, reflux. (d) $SnCl_2$, ethanol, reflux. (e) $(CH_2O)_n$, NaOMe, methanol, reflux. $NaBH_4$, reflux. (f) 4-Dimethylaminobenzoyl chloride, toluene/NEt_3, reflux.

Scheme 2[a]

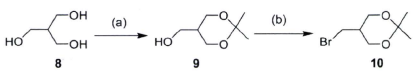

[a] Reagents and conditions: (a) $(CH_3O)_2C(CH_3)_2$, TsOH. (b) CBr_4, PPh_3, pyridine, DCM.

To prepare the amine compound **5**, the nitro group was reduced with $SnCl_2$ in ethanol (yield 93%). Conversion of **5** to the corresponding monomethylamino derivative **6** was achieved by monomethylation with paraformaldehyde and NaOMe (yield 30%). The synthesis outlined in Schemes 2 and 3 was achieved using methods reported previously.[18−22]

The binding experiments were carried out as described previously.[17,23] Assays using Aβ(1−42) aggregates demonstrated that these fluorinated benzofuran derivatives competed with [^{125}I]IMPY to bind β-amyloid plaques with excellent affinity (Table 1).[24,25] Compound **7** with a dimethylaminophenyl moiety in the phenylbenzofuran molecule displayed slightly lower values (higher affinity) than **5** with an aminophenyl moiety or **6** with a monomethylaminophenyl moiety. However, all of the derivatives maintained good binding affinity with K_i values in the nanomolar range. The results strongly support our previous finding that benzofuran derivatives have considerable tolerance for structural modification.[17,18] Among the derivatives with high affinity for Aβ aggregates, **17** was tested further because of the ease with which it could be labeled with ^{18}F.

The ^{18}F-labeled **17** ([^{18}F]**17**) was prepared from a tosyl precursor (**22**) via a nucleophilic displacement reaction with the fluoride anion (Scheme 4).[23] A solution of **22** (1.0 mg) in acetonitrile (200 μL) was added to a reaction vessel containing ^{18}F. The mixture was heated at 120 °C for 10 min. Radiolabeling of the precursor generated [^{18}F]**17** with an average radiochemical yield of 10.0% and radiochemical purity of >99%. The specific activity of [^{18}F]**17** was 242 GBq/μmol. The identity of [^{18}F]**17** was verified by a comparison of the retention time with the nonradioactive compound. Initially, **21** was expected to show similar radiolabeling to **17**. However, the radiolabeling of **21** under the various reaction conditions normally used for ^{18}F radiolabeling gave a radiochemical yield (<0.1%) too low to conduct a subsequent distribution experiment.

To evaluate the uptake of [^{18}F]**17** in the brain, a biodistribution experiment was performed in normal mice (Table 2). [^{18}F]**17** displayed high uptake (5.66% ID/g) at 10 min postinjection, sufficient for PET imaging, and the radioactivity in the brain cleared with time. At 60 min postinjection, the uptake was 2.80% ID/g, indicating a relatively slow washout from the brain. One way to select a ligand with appropriate kinetics in vivo is to use the $brain_{2\,min}/brain_{60\,min}$ ratio as an index to compare the washout rate. Although the $brain_{2\,min}/brain_{60\,min}$ ratio of [^{18}F]**17** (1.0) was still lower than that of [^{11}C]PIB (12.0)[7,8] or [^{18}F]AV-45 (3.80),[14,15] it was much improved as compared to the values for iodinated benzofuran derivatives

DOI: 10.1021/ml100082x | ACS Med. Chem. Lett. 2010, 1, 321–325

Scheme 3[a]

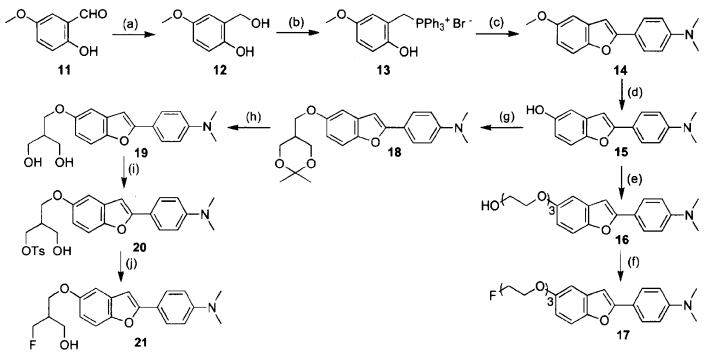

[a] Reagents and conditions: (a) $NaBH_4$, ethanol. (b) Triphenylphosphine hydrobromide, acetonitrile, reflux. (c) 4-Dimethylaminobenzoyl chloride, toluene/NEt_3, reflux. (d) BBr_3/CH_2Cl_2. (e) 2-[2-(2-Chloroethoxy)ethoxy]ethanol, K_2CO_3, DMF, reflux. (f) DAST, DME. (g) 5-(Bromomethyl)-2,2-dimethyl-1,3-dioxane (**10**), K_2CO_3, DMF, 100 °C. (h) HCl, acetone. (i) Tosyl chloride, pyridine, 0 °C. (j) TBAF, THF, reflux.

Scheme 4[a]

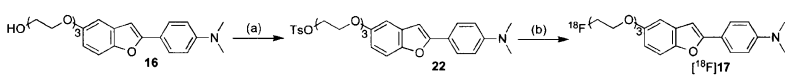

[a] Reagents and conditions: (a) Tosyl chloride, pyridine. (b) Kryptofix222, K_2CO_3, acetonitrile, 120 °C.

Table 1. Chemical Structures and Inhibition Constants of Fluorinated Benzofuran Derivatives

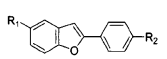

compound	R_1	R_2	K_i (nM)[a]
5	F	NH_2	0.90 ± 0.20
6	F	$NHCH_3$	0.53 ± 0.05
7	F	$N(CH_3)_2$	0.26 ± 0.01
17	$F(CH_2CH_2O)_3$	$N(CH_3)_2$	2.0 ± 0.50
21		$N(CH_3)_2$	1.0 + 0.30

[a] Inhibition constants (K_i, nM) of compounds for the binding of [^{125}I]IMPY to Aβ(1−42) aggregates. Values are the means ± standard errors of the mean for 3−6 independent experiments.

(0.47−0.48) reported previously.[17] Furthermore, among these benzofuran derivatives, the washout rate improved as the lipophilicity decreased (log P values of [^{18}F]**17** and the iodinated benzofuran derivatives were 1.20 and 2.12−2.35, respectively).[17] Thus, lipophilicity is important to improving washout from the brain. To further enhance the washout rate, the synthesis of less lipophilic benzofuran derivatives, for example, by replacing the dimethylamino group with another hydrophilic group, is now under investigation. Uptake in the bone at 60 min was measurable (2.74 % ID/g), suggesting little

Table 2. Biodistribution of Radioactivity after Injection of [^{18}F]**17** in Normal Mice[a]

organ	2 min	10 min	30 min	60 min
blood	1.64 ± 0.07	2.48 ± 0.18	2.68 ± 0.26	3.41 ± 0.56
brain	2.88 ± 0.46	5.66 ± 0.31	3.14 ± 0.26	2.80 ± 0.06
bone	1.19 ± 0.18	1.76 ± 0.13	3.63 ± 1.11	2.74 ± 0.59

[a] Expressed as % of injected dose per gram. Each value represents the mean ± SD for five mice.

defluorination in vivo.[13,19,26] However, the free fluoride was not taken up by brain tissue, and so, interference with the imaging is expected to be relatively minor.

Next, to confirm the specific binding of radiofluorinated ligands to β-amyloid plaques, we performed autoradiographic imaging of [^{18}F]**17** with sections (10 μm) of Tg2576 mouse brain. Tg2576 transgenic mice express human APP695 with the K670N, M671L Swedish double mutation.[27] They show marked Aβ deposition in the cingulated cortex, entorhinal cortex, dentate gyrus, and CA1 hippocampal subfield by 11−13 months of age and have been frequently used to evaluate the specific binding of β-amyloid plaques in experiments in vitro and in vivo.[15,18,19,23] Autoradiographic images of [^{18}F]**17** showed high levels of radioactivity in the brain sections (Figure 2A). Furthermore, the hot spots of [^{18}F]**17** corresponded with those of thioflavin-S, a pathological dye commonly used to stain

DOI: 10.1021/ml100082x | ACS Med. Chem. Lett. 2010, 1, 321–325

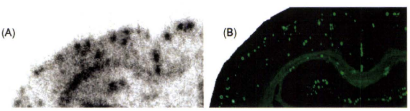

Figure 2. Autoradiography of a section (10 μm) of Tg2576 mouse brain with [^{18}F]**17**. [^{18}F]**17** showed excellent binding to β-amyloid plaques (A). β-Amyloid plaques were confirmed present by staining of the section with thioflavin-S (B).

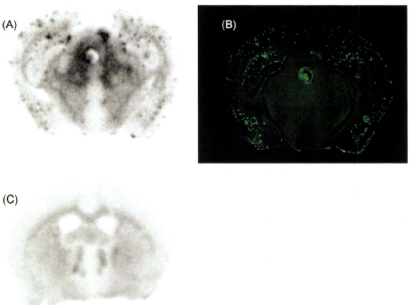

Figure 3. Labeling of β-amyloid plaques in vivo was visualized by autoradiography ex vivo with [^{18}F]**17** in sections of Tg2576 mouse brain (A). The same section was also stained with thioflavin-S (B). Wild-type mouse brain showed no β-amyloid plaques (C).

β-amyloid plaques (Figure 2B). The results suggest that [^{18}F]**17** shows affinity for β-amyloid plaques in the mouse brain in addition to binding synthetic Aβ aggregates.

To further characterize the potential of [^{18}F]**17** as an agent for imaging β-amyloid plaques in living brain tissue, we carried out autoradiography ex vivo in a Tg2576 mouse (36 months, male). The autoradiography showed distinctive labeling of β-amyloid plaques in the brain (Figure 3A), which was confirmed by costaining of the sections with thioflavin-S (Figure 3B). Wild-type mouse brain showed no β-amyloid plaques (Figure 3C). This is consistent with results in vitro showing [^{18}F]**17** to be highly selective in binding to β-amyloid plaques in the brain.

In summary, we produced a series of fluorinated benzofuran derivatives that bind well to Aβ(1−42) aggregates and clearly stain β-amyloid plaques. In experiments in vitro and ex vivo using an animal model of AD, [^{18}F]**17** intensely labeled β-amyloid plaques. These newly synthesized derivatives may become PET radiotracers for imaging β-amyloid plaques in the brain and deserve further investigation by optimizing the substituted groups into the benzofuran backbone.

SUPPORTING INFORMATION AVAILABLE Procedures for the preparation of new fluorinated benzofuran derivatives, in vitro binding assay, in vitro autoradiography using Tg2576 mouse brain sections, and ex vivo autoradiography using Tg2576 mice. This material is available free of charge via the Internet at http://pubs.acs.org.

AUTHOR INFORMATION

Corresponding Author: *To whom correspondence should be addressed. Tel: 81-75-753-4608. Fax: 81-75-753-4568. E-mail: ono@pharm.kyoto-u.ac.jp (M.O.). Tel: 81-75-753-4556. Fax: 81-75-753-4568. E-mail: hsaji@pharm.kyoto-u.ac.jp (H.S.).

Funding Sources: This study was supported by the Program for Promotion of Fundamental Studies in Health Sciences of the National Institute of Biomedical Innovation (NIBIO), a Health Labour Sciences Research Grant, and a Grant-in-Aid for Young Scientists (A) and Exploratory Research from the Ministry of Education, Culture, Sports, Science and Technology, Japan.

REFERENCES

(1) Selkoe, D. J. Alzheimer's Disease: Genes, Proteins, and Therapy. *Physiol. Rev.* **2001,** *81*, 741–766.
(2) Hardy, J.; Selkoe, D. J. The Amyloid Hypothesis of Alzheimer's Disease: Progress and Problems on the Road to Therapeutics. *Science* **2002,** *297*, 353–356.
(3) Selkoe, D. J. Imaging Alzheimer's Amyloid. *Nat. Biotechnol.* **2000,** *18*, 823–824.
(4) Mathis, C. A.; Wang, Y.; Klunk, W. E. Imaging β-Amyloid Plaques and Neurofibrillary Tangles in the Aging Human Brain. *Curr. Pharm. Des.* **2004,** *10*, 1469–1492.
(5) Nordberg, A. PET Imaging of Amyloid in Alzheimer's Disease. *Lancet Neurol.* **2004,** *3*, 519–527.
(6) Ono, M.; Wilson, A.; Nobrega, J.; Westaway, D.; Verhoeff, P.; Zhuang, Z. P. ^{11}C-labeled Stilbene Derivatives as Aβ-Aggregate-Specific PET Imaging Agents for Alzheimer's Disease. *Nucl. Med. Biol.* **2003,** *30*, 565–571.
(7) Mathis, C. A.; Wang, Y.; Holt, D. P.; Huang, G. F.; Debnath, M. L.; Klunk, W. E. Synthesis and Evaluation of ^{11}C-Labeled 6-Substituted 2-Arylbenzothiazoles as Amyloid Imaging Agents. *J. Med. Chem.* **2003,** *46*, 2740–2754.
(8) Klunk, W. E.; Engler, H.; Nordberg, A.; Wang, Y.; Blomqvist, G.; Holt, D. P. Imaging Brain Amyloid in Alzheimer's Disease with Pittsburgh Compound-B. *Ann. Neurol.* **2004,** *55*, 306–319.
(9) Kudo, Y.; Okamura, N.; Furumoto, S.; Tashiro, M.; Furukawa, K.; Maruyama, M.; Itoh, M.; Iwata, R.; Yanai, K.; Arai, H. 2-(2-[2-Dimethylaminothiazol-5-yl]ethenyl)-6-(2-[fluoro]ethoxy)-benzoxazole: A Novel PET Agent for in vivo Detection of Dense Amyloid Plaques in Alzheimer's Disease Patients. *J. Nucl. Med.* **2007,** *48*, 553–561.
(10) Small, G. W.; Kepe, V.; Ercoli, L. M.; Siddarth, P.; Bookheimer, S. Y.; Miller, K. J.; Lavretsky, H.; Burggren, A. C.; Cole, G. M.; Vinters, H. V.; Thompson, P. M.; Huang, S. C.; Satyamurthy, N.; Phelps, M. E.; Barrio, J. R. PET of Brain Amyloid and Tau in Mild Cognitive Impairment. *N. Engl. J. Med.* **2006,** *355*, 2652–2663.
(11) Shoghi-Jadid, K.; Small, G. W.; Agdeppa, E. D.; Kepe, V.; Ercoli, L. M.; Siddarth, P.; Read, S.; Satyamurthy, N.; Petric, A.; Huang, S. C.; Barrio, J. R. Localization of Neurofibrillary Tangles and β-Amyloid Plaques in the Brains of Living Patients with Alzheimer Disease. *Am. J. Geriatr. Psychiatry* **2002,** *10*, 24–35.
(12) Rowe, C. C.; Ackerman, U.; Browne, W.; Mulligan, R.; Pike, K. L.; O'Keefe, G.; Tochon-Danguy, H.; Chan, G.; Berlangieri, S. U.; Jones, G.; Dickinson-Rowe, K. L.; Kung, H. P.; Zhang, W.;

Kung, M. P.; Skovronsky, D.; Dyrks, T.; Holl, G.; Krause, S.; Friebe, M.; Lehman, L.; Lindemann, S.; Dinkelborg, L. M.; Masters, C. L.; Villemagne, V. L. Imaging of Amyloid β in Alzheimer's Disease with ^{18}F-BAY94-9172, A Novel PET Tracer: Proof of Mechanism. *Lancet Neurol.* **2008,** *7*, 129–135.

(13) Zhang, W.; Oya, S.; Kung, M. P.; Hou, C.; Maier, D. L.; Kung, H. F. F-18 Polyethyleneglycol Stilbenes as PET Imaging Agents Targeting Aβ aggregates in the Brain. *Nucl. Med. Biol.* **2005,** *32*, 799–809.

(14) Choi, S. R.; Golding, G.; Zhuang, Z.; Zhang, W.; Lim, N.; Hefti, F.; Benedum, T. E.; Kilbourn, M. R.; Skovronsky, D.; Kung, H. F. Preclinical Properties of ^{18}F-AV-45: A PET Imaging Agent for Aβ Plaques in the Brain. *J. Nucl. Med.* **2009,** *50*, 1887–1894.

(15) Kung, H. F.; Choi, S. R.; Qu, W.; Zhang, W.; Skovronsky, D. ^{18}F Stilbenes and Styrylpyridines for PET Imaging of Aβ Plaques in Alzheimer's Disease. *J. Med. Chem.* **2010,** *53*, 933–941.

(16) Koole, M.; Lewis, D. M.; Buckley, C.; Nelissen, N.; Vandenbulcke, M.; Brooks, D. J.; Vandenberghe, R.; Van Laere, K. Whole-Body Biodistribution and Radiation Dosimetry of ^{18}F-GE067: A Radioligand for in vivo Brain Amyloid Imaging. *J. Nucl. Med.* **2009,** *50* (5), 818–822.

(17) Ono, M.; Kung, M. P.; Hou, C.; Kung, H. F. Benzofuran Derivatives as Aβ Aggregate Specific Imaging Agents for Alzheimer's Disease. *Nucl. Med. Biol.* **2002,** *29*, 633–642.

(18) Ono, M.; Kawashima, H.; Nonaka, A.; Kawai, T.; Haratake, M.; Mori, H.; Kung, M. P.; Kung, H. F.; Saji, H.; Nakayama, M. Novel Benzofuran Derivatives for PET Imaging of β-Amyloid Plaques in Alzheimer's Disease Brains. *J. Med. Chem.* **2006,** *49*, 2725–2730.

(19) Zhang, W.; Oya, S.; Kung, M. P.; Hou, C.; Maier, D. L.; Kung, H. F. F-18 Stilbenes as PET Imaging Agents for Detecting β-Amyloid Plaques in the Brain. *J. Med. Chem.* **2005,** *48*, 5980–5988.

(20) Yuan, W.; Berman, R. J.; Gelb, M. H. Synthesis and Evaluation of Phospholipid Analogues as Inhibitors of Cobra Venom Phospholipase A2. *J. Am. Chem. Soc.* **1987,** *109*, 8071–8081.

(21) Cox, D. P.; Terpinski, J.; Lawrynowicz, W. "Anhydrous" Tetrabutylammonium Fluoride: A Mild but Highly Efficient Source of Nucleophilic Fluoride Ion. *J. Org. Chem.* **1984,** *49*, 3216–3219.

(22) Xu, B.; Stephens, A.; Kirschenheuter, G.; Greslin, A. F.; Cheng, X.; Sennelo, J.; Cattaneo, M.; Zighetti, M. L.; Chen, A.; Kim, S. A.; Kim, H. S.; Bischofberger, N.; Cook, G.; Jacobson, K. A. Acyclic Analogues of Aaenosine Bisphosphates as P2Y Receptor Antagonists: Phosphate Substitution Leads to Multiple Pathways of Inhibition of Platelet Aggregation. *J. Med. Chem.* **2002,** *45*, 5694–5709.

(23) Ono, M.; Watanabe, R.; Kawashima, H.; Cheng, Y.; Kimura, H.; Watanabe, H.; Haratake, M.; Saji, H.; Nakayama, M. Fluoro-Pegylated Chalcones as Positron Emission Tomography Probes for in vivo Imaging of β-amyloid Plaques in Alzheimer's Disease. *J. Med. Chem.* **2009,** *52*, 6394–6401.

(24) Kung, M. P.; Hou, C.; Zhuang, Z. P.; Skovronsky, D.; Kung, H. F. Binding of Two Potential Imaging Agents Targeting Amyloid Plaques in Postmortem Brain Tissues of Patients with Alzheimer's Disease. *Brain Res.* **2004,** *1025*, 98–105.

(25) Kung, M. P.; Hou, C.; Zhuang, Z. P.; Cross, A. J.; Maier, D. L.; Kung, H. F. Characterization of IMPY as a Potential Imaging Agent for β-Amyloid Plaques in Double Transgenic PSAPP Mice. *Eur. J. Nucl. Med. Mol. Imaging* **2004,** *31*, 1136–1145.

(26) Stephenson, K. A.; Chandra, R.; Zhuang, Z. P.; Hou, C.; Oya, S.; Kung, M. P.; Kung, H. F. Fluoro-Pegylated (FPEG) Imaging Agents Targeting Aβ Aggregates. *Bioconjugate Chem.* **2007,** *18*, 238–246.

(27) Hsiao, K.; Chapman, P.; Nilsen, S.; Eckman, C.; Harigaya, Y.; Younkin, S.; Yang, F.; Cole, G. Correlative Memory Deficits, Aβ Elevation, and Amyloid Plaques in Transgenic Mice. *Science* **1996,** *274*, 99–102.

DOI: 10.1021/ml100082x | *ACS Med. Chem. Lett.* **2010,** *1*, 321–325